2023

Assessment Of The Interplay Between Regional **β**-Amyloid Burden And White Matter Hyperintensities On Cognition And Default Mode Network In Clinically Normal Older Participants

Doaa G. Ali
University of Kentucky, doaagamal.md@gmail.com
Digital Object Identifier: https://doi.org/10.13023/etd.2023.035

Recommended Citation

STUDENT AGREEMENT:

I represent that my thesis or dissertation and abstract are my original work. Proper attribution has been given to all outside sources. I understand that I am solely responsible for obtaining any needed copyright permissions. I have obtained needed written permission statement(s) from the owner(s) of each third-party copyrighted matter to be included in my work, allowing electronic distribution (if such use is not permitted by the fair use doctrine) which will be submitted to UKnowledge as Additional File.

I hereby grant to The University of Kentucky and its agents the irrevocable, non-exclusive, and royalty-free license to archive and make accessible my work in whole or in part in all forms of media, now or hereafter known. I agree that the document mentioned above may be made available immediately for worldwide access unless an embargo applies.

I retain all other ownership rights to the copyright of my work. I also retain the right to use in future works (such as articles or books) all or part of my work. I understand that I am free to register the copyright to my work.

REVIEW, APPROVAL AND ACCEPTANCE

The document mentioned above has been reviewed and accepted by the student's advisor, on behalf of the advisory committee, and by the Director of Graduate Studies (DGS), on behalf of the program; we verify that this is the final, approved version of the student's thesis including all changes required by the advisory committee. The undersigned agree to abide by the statements above.

<div align="right">

Doaa G. Ali, Student

Dr. Gregory A. Jicha, Major Professor

Dr. Clair Clark, Director of Graduate Studies

</div>

Title

Assessment Of The Interplay Between Regional β-Amyloid Burden And White Matter Hyperintensities On Cognition And Default Mode Network In Clinically Normal Older Participants.

_____

DISSERTATION

_____

A dissertation submitted in partial fulfillment of the
requirements for the degree of Doctor of Philosophy in the
College of Medicine
at the University of Kentucky

By
Doaa G. Ali
Lexington, Kentucky
Director: Dr. Gregory A. Jicha, Professor of Neurology
Lexington, Kentucky
2023

ABSTRACT OF DISSERTATION

Assessment Of The Interplay Between Regional β-Amyloid Burden And White

Matter Hyperintensities On Cognition And Default Mode Network In Clinically Normal

Older Participants**.**

Objective: Alzheimer's disease (AD) and subcortical vascular dementia are considered the most common pathologic contributors to dementia in the aging population. Both frequently coexist in over 80% of community dwelling adults with dementia. The neuropathological development of AD arguably begins with β-amyloid (Aβ) deposition in the brain. This series of studies aims to test the hypothesis that early focal regional amyloid deposition in the brain is associated with cognitive performance in specific cognitive domain scores in preclinical AD (pAD) (study1). Since mixed dementia is widely recognized as the norm rather than the exception, the second study aimed to explore the relation between regional and global Aβ and WMH with core cognitive function (executive function (EF) and memory) scores in cognitively normal (CN) older adults (study2). Finally, the relationship between WMH and Aβ is strongly determined by the spatial distribution of the two pathologies, so the third study aimed to quantify Aβ in Default mode network (DMN) regions to examine whether cerebral small vessels disease (SVD) disruption of connectivity affects Aβ deposition in disconnected DMN regions (study3).

Method: Global and regional Standard Uptake Value ratios (SUVr) from Aβ-PET, WMH volumes from MRI FLAIR images, and cognitive test scores were analyzed across a sample of CN participants. Linear regression models adjusted for age, sex and education used to assess the relationships between regional SUVr and cognitive test scores across 99 CN from Sanders Brown Center on Aging (study1). Moderation, and mediation modeling were used to define the interplay between global, regional Aβ and WMHs measures in relation to EF and memory composite scores outcomes at baseline and after approximately 2 years across a sample of 714 CN from the Alzheimer's Disease Neuroimaging Initiative ADNI (study2). The association of WMH volume in anatomically defined white matter tracts of atlas-based fiber tract with Aβ SUVr specifically in connected cortical regions within DMN was tested across sample of 74 CN from ADNI3.

Results: EF performance was associated with increased regional SUVr in the precuneus and posterior cingulate regions only ($p<0.05$). The moderation regression analysis showed additive effects of Aβ and WMH over baseline memory and EF scores ($p =0.401$ and 0.061 respectively) and synergistic effects over follow-up EF ($p < 0.05$). Through mediation analysis, the data from study 2 showed that WMH affects, mediated by global and regional amyloid burden, are responsible for baseline cognitive performance deficits in memory and EF. Finally, the regression analysis from study 3 demonstrated that increased WMH

volumes in superior longitudinal fasciculus (SLF) was associated with increased regional SUVr in inferior parietal lobule (IPL) ($p<0.05$).

Conclusion: While the prevailing view in the field suggests that memory performance is the earliest clinical hallmark of AD, the present data demonstrate that changes in EF, mediated by Aβ deposition in the precuneus and posterior cingulate may precede memory decline in pAD. After adding the second key driver of cognitive decline in CN, the finding suggested that WMH dependent changes in baseline cognitive performance are related to direct effect of WMH and an indirect effect through both global and regional Aβ burden. Further studies are needed to show the longitudinal influences of WMH on Aβ distributions in participants with mixed dementia.

Doaa G. Ali
(Name of Student)

[01/21/2023]
Date

Assessment Of The Interplay Between Regional β-Amyloid Burden And White Matter Hyperintensities On Cognition And Default Mode Network In Clinically Normal Older Participants.

By
Doaa G. Ali

Dr. Gregory A. Jicha
Director of Dissertation

Dr. Clair Clark
Director of Graduate Studies

[01/21/2023]
Date

DEDICATION

To my sole inspiration and my soul mate. "My husband" The one who always believed
in me.
To my loving mother and father.
To my daughter and son.

ACKNOWLEDGMENTS

Finally, I would like to thank my family for their support. To my amazing husband, Dr. Moamen Gabr, thank you for providing unconditional support and for always pushing me to do my best. To my parents who I owe most of my success to them.

TABLE OF CONTENTS

LIST OF TABLES

LIST OF FIGURES

CHAPTER 1.   INTRODUCTION

1.1   Alzheimer's disease (AD) and Vascular cognitive impairment and dementia (VCID)

Alzheimer's disease (AD) is the most common neurodegenerative cause of dementia. The pathological hallmarks of AD include but are not limited to extracellular amyloid plaques containing abnormal aggregates of amyloid-beta (Aβ) protein, intracellular neuronal fibrillary tangles (NFTs) composed of hyperphosphorylated tau protein, synaptic loss, neuronal death, mitochondrial dysfunction, oxidative stress, metabolic dysregulation, and neuroinflammation. Aβ occurs many years before the overt detection of cognitive decline (representing the research construct of preclinical Alzheimer's disease (pAD)).[1, 2]. It is challenging to detect early Aβ burden in pAD as it is often low or focal at this stage of disease [3]. Aβ deposition develops over time in discrete regions of the brain in a temporally progressive manner [4], from temporobasal and frontomedial areas, to the remaining associative neocortex, to primary sensory-motor cortex, the medial temporal lobe, and finally the striatum [5]. Global Aβ burden assessment in pAD is likely suboptimal and may miss the earliest signs of Aβ pathology without consideration of the temporal progression of regional Aβ deposition [3].

Vascular cognitive impairment and dementia (VCID) is the second most common cause of dementia after AD corresponding to about 20 % of cases, it received high attention as a modifiable factor for dementia [6-8]. VCID is characterized by cerebral hemodynamic alteration and the underlying mechanisms include large and small vessel diseases and decrease cerebral blood flow [9]. Pathological and neuroimaging studies have pinpointed brain parenchymal lesions that are associated with VCID [8]. The underlying neuropathological lesions help classify VCID into three major categories caused by: strategic infarcts, multiple small (lacunar) and or larger vessel infarcts, and subcortical small vessel ischemic disease, which is considered the most common cause of VCID [10]. Advances in multimodal biomarkers like neuroimaging, cerebrospinal fluid (CSF), and blood biochemical analysis contribute to stratifying risk, prognosis, and in the development of treatment plans for VCID patients [11, 12]. Neuroimaging modalities such as magnetic resonance imaging (MRI) and positron emission tomography (PET) are used to determine the extent and the location of vascular injury and provide structure and function information [9, 13].

Diagnosis of dementia relies on a wide range of neuroimaging modalities [14]. MRI is the key neuroimaging modality in VCID [15] and is used to analyze the morphological alterations

that occur in both white and grey matter. Different acquisition sequences can be used to identify the structural and even biologic processes contributing to VCID. Structural T1 identifies area of encephalomalacia from ischemic injury, T2 and fluid-attenuated inversion recovery (FLAIR) imaging identifies area of injury that have not yet progressed to overt encephalomalacia [16], diffusion tensor imaging (DTI) identifies abnormalities in white matter tracts of the brain affected by ischemia, susceptibility-weighted imaging detects areas of active and or prior hemorrhage, arterial spin labeling can detect brain perfusion deficits [17], and spectroscopy can detect biochemical changes associated with regional brain injury and inflammation [18]. The inclusion of quantitative metrics for research applications, is slowly being incorporated into clinical care paradigms, but primarily serves as a toll for research discoveries. Quantitative MRI analysis uses both automated and semi-automated techniques afforded by specialized hardware and software, but while revealing, is also associated with extensive post-acquisition processing, which currently limits its widespread use in clinical practice [19].

1.2   Beta-amyloid (Aβ) protein deposition and Positron Emission Tomography (PET) scans

Brain Aβ deposition can be measured using different radiotracers, including 18F-florbetapir PET. Aβ -PET scans enable quantitative evaluation of regional Aβ elevations in pAD, unlike CSF, which can measure summative brain changes in A□, but cannot provide regional information. The standard quantification technique for Aβ -PET imaging is comparing regional uptake to a reference region. The selection of target and reference regions directly affects the sensitivity of Standardized Uptake Value Ratio (SUVr) quantification. Neuroimaging studies examining the use of different reference regions in analyzing amyloid burden have shown that whole cerebellum, and cerebellar gray matter but not pons nor white matter, are appropriate reference regions in both AD and subcortical vascular dementia [20, 21] As such, the cerebellum is considered a gold standard reference region for A□ burden analyses [22-25]. Not only because it met the assumptions of a standard reference region like having the same tissue characteristics as the target tissue, and showing longitudinal stability [26, 27], but also because autopsies studies had shown low levels of amyloid plaques in this brain region [22, 23].

The integration of PET into our brain imaging toolkit affords an opportunity to improve early and differential diagnosis of many neurodegenerative diseases, through its ability to detect molecular signatures depending on the tracer used [28]. Co-registration of brain PET and MRI data allows for precisely identifying anatomical structures and lesions by providing accurate

parcellation of the brain's gray (GM) and white matter (WM) [29]. Automated quantification of PET and MRI images requires using a series of registrations: first rigid registration between the PET scan and a corresponding T1-weighted MRI scan, then nonlinear registration between the corresponding T1-weighted MRI and a common template space, finally the regions of interest defined in the common template space are then backward-propagated to the subject scans [30]. Many tools could be applied for PET-MRI registration (e.g., tools in FSL, FreeSurfer, ANTs), but *spm_coreg* is most popular for amyloid PET studies [20, 31-34]. Several methods for amyloid PET quantification without MRI co=registration are in active clinical and research use [35-38]. This method of quantification poses many difficulties in interpretation of the data derived due to a lack of anatomic information related to the low resolution of PET imaging, partial volume effects [39-41], and the variability in intensity distribution across brain regions. CT scans are typically performed in the setting of PET to deal with many of the issues, but are suboptimal when using images outside of the structural T1 images, such as those needed to examine VCID and PET in combination. As such, co-registration with MRI is ideal for regional quantification of PET abnormalities that enhance clinical research.

1.3   The impact of Aβ on cognition in clinically normal participants

It is challenging to determine the clinically significant cognitive change in pAD, and results often differ across studies [42-55]. The expression of symptoms may differ dramatically among participants with pAD, and the extent and distribution of amyloid pathology in the brain needs to be considered when analyzing the impact of early preclinical A□ changes. One recent study has been shown that slight deterioration in cognitive function occurred with subthreshold levels of global A*β* in cognitively normal participants [56]. Other studies of this type are scarce in the field. The quantitative evaluation of regional Aβ deposition and its relation to cognitive decline in pAD has not been fully described in the literature and relatively few studies have explored the association between specific cognitive functions and early preclinical Aβ deposition in discrete brain regions

1.4   The relation between cerebral SVD, Aβ, and cognition

Aβ deposition in the brain and its effect on cognitive decline should not be studied in isolation, but in the context of coexisting pathology. Autopsy studies have shown that brain Aβ frequently co-occurs with cerebral small vessel disease (SVD) suggesting an intreplay of these pathologic insults [57-60]. SVD refers to a varied group of diseases that affect the cerebral small

arteries and microvessels [61, 62]. Features of SVD seen on neuroimaging include recent subcortical infarcts, white matter hyperintensities (WMH), lacunes, prominent perivascular spaces, and cerebral microbleeds, frequently associated with cerebral atrophy [63].

Understanding the biological and pathological changes of white matter (WM) that occur in SVD is critical for identifying accurate outcome measures in future studies and clinical trials [64]. The pathological change of WM starts with chronic hypoxia, which leads to axonal loss, demyelination, increased inflammatory infiltrate, and gliosis [65]. These changes are detected as hyperintense signals on FLAIR MRI images [13]. WM damage is not always limited to the initially visible lesions (WMH) in FLAIR scan; there are subtle changes that occur in the normal-appearing white matter like decreased myelin and/or axonal density leading to microstructural WM disruption [66]. Through DTI, microstructural WM disruption could be assessed in vivo by measuring the rate and direction of diffusion of water molecules trapped in neural tissue [67]. FLAIR and DTI seem to be appropriate predictors of white matter injury. FLAIR studies may fail to capture the true degree and extent of white matter injury but are easy to interpret in clinical practice [64]. Semi-automated and automated quantification techniques of WMH volumes vary across studies and research sites [68-72]. Generally, all of them use the same basic concepts regardless the difference in software and algorithms, which include: 1) image registration, 2) nonbrain tissue stripping, 3) intensity estimation and thresholding, and 4) manual editing (as deemed necessary) [70].

Irrespective of the relationships that may exist between Aβ and SVD, it is clear that co-occurrence of Aβ and WMH [73] increases the risk of dementia, suggesting an additive or even a possible synergistic effect [74, 75]. Previous studies evaluating the relationship between brain Aβ, WMH, and cognition have shown conflicting results [60]. Most of them have demonstrated an independent and additive effect of brain Aβ and WMH [59, 76-78] while; few studies had shown interaction effect between brain Aβ and higher WMH volumes on specific cognitive domains [79-81]. Studying the effect of Aβ and WMH on cognition without emphasizing the importance of lesion location may lead to a premature dismissal of hypotheses assessing the functional interactions between these two major pathologies.

1.5   The association between Cerebral SVD to AD

Despite the findings from the recent studies supporting the significant role of WMH in cortical Aβ accumulation and AD development [82-88], the "amyloid cascade hypothesis" [89] still drives ongoing basic and clinical research discoveries and has dominated the field in regards to clinical trials in AD [90, 91]. This may be because the underlying mechanistic linking of WMH to AD pathology is still unclear, and it is also not fully understood if WMH are merely additive to AD pathology or whether WMH may actually initiate or accelerate AD pathology. The pathology underlying individual cases of AD are likely quite varied based on the regional distribution of Aβ deposition, and may additionally be influenced by pre-existing and or accumulating WMH pathology [92]. The pathological interaction between WMH and AD pathology within discrete white matter tracts and connected cortical regions has not been closely investigated but deserves in depth investigation.

WM alterations (including overt WMH and microstructural WM disruption) have been largely identified in specific subcortical neuroanatomic regions that are connected with often distant cortical regions harboring the greatest amount of AD pathology [92-94]. The association between regional distribution of WMHs and global Aβ has been studied initially in a few cross-sectional studies, that have suggested a greater posterior involvement of WMH in AD [92, 95-99]. Of interest, the tracts with the remarkable WM microstructure alternation (the main cingulum bundle, and the superior longitudinal fasciculi) are anatomically connected to the brain regions that are affected with Aβ pathology at the earliest stages of disease within the Default Mode Network (DMN) [100-102].

1.6   Chapters organization: this thesis consists of 5 chapters that are organized as fellow

Chapter 1 presents an introduction to basic concepts necessary to understand the brain change in the pAD stage and its diagnosis, which based on biomarker positivity. Also in this chapter is an introduction to explain the effect of WMH on Aβ and the effect of the two primary drivers of preclinical dementia on cognition.

Chapter 2 present a study that aims to test the hypothesis that early focal regional amyloid deposition in the brain is associated with cognitive performance in specific cognitive domain scores in pAD. Global and regional standardized uptake value ratios (SUVr) from 18f-florbetapir PET/CT scanning were determined across a sample of 99 clinically normal

participants with Montreal Cognitive Assessment (MoCA) scores ≥ 23. Relationships between regional SUVr and cognitive test scores were analyzed using linear regression models adjusted for age, sex and education. Participants were divided into two groups based on SUVr in the posterior cingulate and precuneus gyri (SUVR≥1.17). Between group differences in cognitive test scores were analyzed using ANCOVA models. Executive function performance was associated with increased regional SUVr in the precuneus and posterior cingulate regions only. We also found no significant associations between memory and Aβ-PET SUVr in any regions of the brain. We conclude that increased Aβ deposition in the precuneus and posterior cingulate (the earliest brain regions affected with Aβ pathology) is associated with changes in executive function that may precede memory decline in pAD.

Chapter 3 aims to explore the relation between regional and global Aβ and WMH with cognitive performance in cognitively normal (CN) older adults at baseline, and further examine the relation between baseline WMH and regional Aβ deposition in relation to future cognitive performance. Moderation, and mediation modeling were used to define the interplay between global, regional Aβ and WMHs measures in relation to cognitive (memory and EF) composite score outcomes at baseline and after approximately 2 years across a sample of 714 clinically-normal (Mini-Mental State Examination (MMSE) ≥ 26), aged participants from the Alzheimer's Disease Neuroimaging Initiative (ADNI2). The moderation regression analysis showed additive effects of Aβ burden and WMH over baseline cognitive performance and synergistic effects over longitudinal EF only. Through mediation analysis, we demonstrated that the influence of WMHs over baseline cognitive performance is mediated by global and regional Aβ. We conclude that Aβ and WMHs contribute to baseline cognitive performance independently while WMH volumes exert effects on baseline cognitive performance directly and through influences on Aβ accumulation.

Chapter 4 aims to test the hypothesis that cerebral SVD is associated with increase Aβ distribution within areas of the brain disconnected by the cerebral SVD that lie within the DMN hit hardest and earliest in the pathogenesis of AD in even cognitively normal older adults. We explored the association of WMH volumes in major fiber tracts from DMN regions using Johns Hopkins University International Consortium for Brain Mapping probabilistic fiber tract atlas (JHU-ICBM-tracts) with Aβ-PET SUVr in cortical DMN regions across a sample of 72 clinically-normal MMSE ≥ 26, aged participants from the Alzheimer's Disease Neuroimaging Initiative (ADNI3). The regression analysis demonstrated that increased WMH volumes in

superior longitudinal fasciculus (SLF) was associated with increased regional SUVr in inferior parietal lobule (IPL) (p<0.05). The findings suggest that the relation between Aβ and SVD in influencing executive function in pAD is partially driven directly by WMH and is additionally contributed to by WMH injury that accelerates Aβ deposition ultimately leading to the deficits in executive function seen in pAD.

Chapter 5 presents a summary of this dissertation and points out future perspectives. This thesis includes a diverse set of work and experiments with a primary focus on the importance of using regional amyloid quantification rather than using global measure of Aβ. Another main objective of this thesis is exploring how regional Aβ and WMH interact on a biological level.

CHAPTER 2.   Amyloid-PET levels in the Precuneus and Posterior Cingulate Cortices are Associated with Executive Function Scores in Preclinical Alzheimer`s Disease Prior to Overt Global Amyloid Positivity

2.1   Introduction

Dementia is a major and increasing global health challenge with 40–50 million people currently living with dementia worldwide [103]. Alzheimer's disease (AD) is the most common cause of dementia corresponding to about 60% of cases [104]. The neuropathological development of AD arguably begins with β-amyloid (Aβ) deposition in the brain, which occurs many years before the appearance of cognitive decline (preclinical Alzheimer's disease (pAD)) [1, 2], and has been identified as a risk factor for subsequent dementia [105, 106]. The diagnosis of pAD is based on biomarker positivity using diagnostic tests such as amyloid tracer-based positron emission tomography (Aβ-PET) and cerebral spinal fluid (CSF) measures of Aβ [107].

It is challenging to detect clinically significant cognitive change in pAD, and results have been variable across studies [42-49, 51-55]. Although Aβ deposition is a gradual process [108] that develops over time in discrete regions of the brain in a temporally progressive manner [4], the majority of published studies have focused on global rather than regional measures of Aβ positivity. One recent study, however, demonstrated that patients with early focal Aβ deposition had clinical features that differed from persons with more diffuse global Aβ deposition, suggesting that further study is needed [109]. Another recent study has shown that preclinical Aβ accumulation in the precuneus, medial orbitofrontal, and posterior cingulate cortices can be detected in participants prior to the development of abnormal CSF Aβ42 or global Aβ PET scan positivity [102, 110]. Limitations of recent studies on regional quantification of amyloid pathology also include a primary focus on memory domain impairment rather than examining a broader array of cognitive domain involvement [111-113]. Additionally, previous studies examining relationships between regional Aβ deposition and different domains of cognition have largely focused on comparing cognitively normal participants to mild cognitively impaired or AD patients, but notably did not include pAD participants [114-116]. As early identification of pAD is an important goal for the field, an accurate and thorough understanding of the cognitive and brain changes accompanying this stage of disease is critical [117].

The main objective of this study was to test the hypothesis that early focal regional amyloid deposition in the brain is associated with preclinical cognitive decline in specific cognitive domains (memory & executive function) in elderly cognitively intact persons (pAD).

2.2   Methods

2.2.1   Study design and participants

This cross-sectional study included review of the neuroimaging and clinical data from participants who underwent F-florbetapir PET/CT scanning between 2015 and 2020 at the Sanders Brown Center on Aging. This study was approved by the University of Kentucky (UK) Institutional Review Board (IRB), and a signed IRB consent was obtained from each subject prior to participation.

Inclusion criteria included the availability of:

- Complete demographic information (age, sex, and years of education)

- Neurocognitive function that covered major cognitive functions [103], the Montreal Cognitive Assessment (MoCA) [104], The Trail Making Test (TMT), and California Verbal Learning Test - II (CVLT-II) [105],

- Cognitively intact participants with a MoCA score ≥23 to exclude participants with mild cognitive impairment (MCI) or dementia, as described previously [106].

2.2.2   Acquisition of Flobetapir PET/CT

For each scan, the participant received a single intravenous administration of approximately 370 MBq (10 mCi) of florbetapir F 18 (fast intravenous push). The injection of the imaging agent was followed by a saline flush. After an uptake period of 50 min, participants were positioned in a head stabilization unit designed for PET/CT scanners. All PET/CT scans were performed on a Siemens Biograph TruePoint 6-slice (Siemens Healthcare, Erlangen, Germany). Low resolution CT images of the head will be acquired (120 kVp, FOV 50 cm, pitch 0.55, 0.5 s

rotation time, slice thickness 4 mm, care dose). PET images of the brain were then collected for a 20-min, 3D emission scan. The emission images are reconstructed using 256×256 matrix and all-pass filter.

All F-florbetapir PET/CT images were analyzed using dedicated viewing software (Syngo.via®; Siemens) [107]. Siemens *Syngo.VIA* Amyloid Plaque (Siemens Medical Solutions Inc., Malvern, PA, USA) software package was used for neurological evaluations of PET/CT. Quantitative parametric analysis was performed with Database Comparison software (Siemens Medical Solutions, Inc.) that automatically identifies regions of interest (ROIs) based on the analysis method used by Fleisher [108]. The regions (frontal, temporal, parietal, anterior cingulate, posterior cingulate, and precuneus) were selected based on the analysis described by Fleisher and Clark in the use of florbetapir-PET in β-amyloid imaging analysis [108, 109]. Since the occipital region is significantly affected more than any other region in cerebral amyloid angiopathy, we exclude this region from the analysis [110, 111]. The mean uptake of ROIs was calculated. Standardized uptake value (SUV) is a semi quantitative measure of the intensity of radiotracer activity at each voxel [112]. The mean SUV of each region is normalized to the mean SUV of the cerebellum (SUVr) (SUVr = SUV target/ SUV reference) [113].

A threshold of SUVrs greater than or equal to 1.17 was used to reflect pathological levels of amyloid associated with MCI and AD [108, 114, 115]. We choose to focus on the mean score of posterior cingulate and precuneus gyri SUVrs as these regions are among the earliest brain regions of amyloid deposition [25, 116-118]. The participants were divided into two groups (pAD and control group) based on SUVr in the posterior cingulate and precuneus gyri (SUVr≥1.17).

2.2.3   Neuropsychological cognitive test

We examined cognitive test scores that assess major cognitive functions, including global cognition with the MoCA [104] , processing speed, attention and executive function with TMT [119] , and memory function with the CVLT-II [105]. The MoCA is a brief test of cognitive function that assesses visuospatial, naming, attention, language, abstraction, delayed recall and orientation. Total score is generated by summing scores across all of these domains [120]. TMT is a neuropsychological test of visual attention and task switching. In Part A, participants were asked to link numbered points randomly distributed on a sheet of paper in ascending order according to numbers. In Part B, the participants were asked to link numbers and letters

alternately. The time of each test performance was measured, the number of errors were counted, and the difference in times: B-A was calculated [121]. CVLT-II is a widely used measure of verbal episodic learning and memory. A list of 16 items organized into four semantic categories are presented to the subject over five immediate recall trials, free and category cued recall is tested after short and longer (20-min) intervals. We chose to focus on the CVLT-II learning component of the test, which is the sum of the five immediate recall trials, as well as free delayed recall scores.

2.2.4 Statistical analysis

Statistical analyses were performed in IBM SPSS Statistics v28. Significance was set at $P < .05$, with Bonferroni correction based on the number of cognitive tests as a dependent variable.

In the first analysis, we used ANCOVA to evaluate whether the means of score of cognitive tests are equal across different levels of posterior cingulate and precuneus SUVr, while statistically controlling for the covariates (age, sex, and education). We tested the homogeneity to make sure the values of covariates did not vary and equal over all the two groups using ANOVA. Differences in performance on the neuropsychological cognitive tests between pAD and controlled group were tested using one-way ANCOVA after adjustment for covariates. The difference in the scores of cognitive function tests across different level of global SUVr were assessed using ANCOVA again.

In the second analysis, linear regression adjusted for age, sex and education was used to explore the relationship between regional SUVr (independent variables) and the cognitive function scores (dependent variable). Due to high co-linearity between regional SUVr measures regressions were initially run separately for each region. This process was repeated for each cognitive test (TMT B, TMT B-A, MoCA, and CVLT (learning score, short free delay recall, and long free delay recall)). Relationships between regional SUVr from multiple regression from the prior step and MoCA domain scores were analyzed using linear regression models adjusted for age, sex, and education.

2.3   Results

        The demographic, clinical and imaging characteristics of the sample are provided in table 2.1. Briefly, the sample included 68 women and 31 men with a mean age of 74.2 ± 6.3 years, education 16.7 ± 2.6 years. Posterior cingulate and precuneus SUVrs ranged from 0.85 to 2.43 in this study cohort.

2.3.1   The differences of the demographic and cognitive measures, between the preclinical and control group

        Dividing the cohort into two groups based on SUVr of posterior cingulate and precuneus SUVr > 1.17, allowed an analysis of 45 participants in the pAD group and 54 participants in the control group. Between-group differences on demographic variables were not significant, including sex at birth, where a chi-square test showed non-significant between group differences (p value $= 0.83$; data not shown in Table 1). Cognitive and imaging measures that clearly defined the groups as distinct are presented in Table 2.1

Table 2.1The differences of the demographic and cognitive measures, between the preclinical and control group

	pAD		Control		
	Mean	SD	Mean	SD	p
Age	75.08	7.01	73.46	5.6	0.203
Education	16.8	2.93	16.57	2.39	0.69
MoCA	26.2	1.85	27	1.83	0.036*
TMT A	34.51	11.73	33.6	10.91	0.92
TMT B	92.07	38.41	73.36	27.6	0.011*
TMT B-A	57.56	31.62	39.75	21.3	0.002**
CVLT-II Total Learning	47	11.67	47.83	10.89	0.7
CVLT-II Short-Delay Free	9.91	4.25	11.3	3.57	0.089
CVLT-II Long-Delay Free	9.98	3.99	11.39	3.53	0.072

No significant between group differences on demographic variables were seen between pAD (n=45) and control groups (n=54). Significant between group differences were seen for MoCA, TMT B, and TMT B-A scores. Abbreviations: SD: standard deviation; SUVr: Standardized Uptake Value ratio; AD: ''Alzheimer's Disease; MoCA: Montreal Cognitive Assessment; TMT: Trail Making Test; CVLT: California Verbal Learning Test –II.
*0.05 level significance

Figure 2.1 differences of the demographic and cognitive measures, between the preclinical and control group

Figure A   Figure B
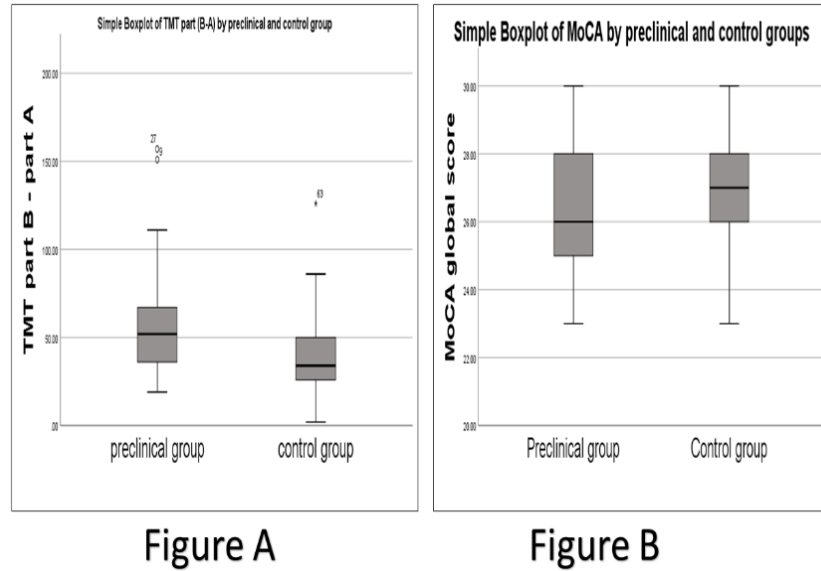
Comparison of cognitive measure scores Trail Making Test (TMT) part B-A, and The Montreal Cognitive Assessment (MoCA) among preclinical group and control group based on SUVr of posterior cingulate and precuneus SUVr > 1.17 after adjusted for age, education, and sex. Figure A shows the difference in the scores of TMT part B-A between the groups. Box and whisker plots of the MoCA score (Figure B) show medians, lower to upper quartile, and lines extending from minimum to maximum values

2.3.2   The association between regional Aβ-PET SUVr and cognitive test scores

In the second set of analyses (shown in Table 2.2), linear regression analysis was used with each region (Aβ-PET SUVr of independent frontal, parietal, temporal, anterior cingulate, posterior cingulate, and precuneus cortical regions) used as independent variables and cognitive test scores as a dependent variable to explore associations of amyloid deposition in regions of the brain with MoCA, TMT, and CVLT. Age, sex, and education were entered as covariates in the analysis. The adjusted linear regression analyses demonstrated that increased regional SUVr in the precuneus and posterior cingulate regions only were associated with reduced global MoCA score and TMT B-A scores (shown in figure 2.2) ($p<0.05$).

Table 2.2 Testing the independent effect of regional Aβ SUVr burden on cognitive function test scores

Cognitive Function test	Regional SUVr	Coeff. β (p-value)	Adjusted R square
MoCA	Frontal SUVr	-1.01(.172)	.052
	Parietal SUVr	-1.141(.176)	.052
	Temporal SUVr	-1.244(.157)	0.054
	PCC & precuneus SUVr	-1.612(.023)	0.086
	Anterior cingulate SUVr	-0.479(0.434)	0.039
TMT part A	Frontal SUVr	-1.92(0.671)	0.028
	Parietal SUVr	1.31(0.799)	0.027
	Temporal SUVr	-1.49(0.781)	0.027
	PCC. & precuneus SUVr	0.804(0.854)	0.027
	Anterior cingulate SUVr	-0.26(0.944)	0.026
TMT part B	Frontal SUVr	11.231(0.401)	0.093
	Parietal SUVr	16.833(0.268)	0.098
	Temporal SUVr	9.57(0.547)	0.089
	PCC & precuneus SUVr	20.971(0.102)	0.112
	Anterior cingulate SUVr	9.25(0.401)	0.093

Table 2.2 continued

TMT (B-A)	Frontal SUVr	13.15(0.228)	0.108
	Parietal SUVr	15.526(0.210)	0.109
	Temporal SUVr	11.066(0.393)	0.100
	PCC & precuneus SUVr	20.17(0.04)	0.130
	Anterior cingulate SUVr	9.507(0.290)	0.104
CVLT (learning score)	Frontal SUVr	-1.38 (0.772)	0.105
	Parietal SUVr	1.83(0.736)	0.106
	Temporal SUVr	0.07(0.991)	0.105
	PCC & precuneus SUVr	-2.59(0.6)	0.107
	Anterior cingulate SUVr	0.17(0.965)	0.105
CVLT (short free delay recall)	Frontal SUVr	-0.66(0.692)	0.124
	Parietal SUVr	-0.57(0.764)	0.123
	Temporal SUVr	-1.44(0.484)	0.127
	PCC & precuneus SUVr	-1.63(0.343)	0.131
	Anterior cingulate SUVr	-0.06(0.965)	0.123
CVLT (long free delay recall)	Frontal SUVr	-1.70(0.273)	0.180
	Parietal SUVr	-1.75(0.320)	0.178

Table 2.2 continued

CVLT (long free delay recall)	Temporal SUVr	-2.73(0.155)	0.188
	PCC & precuneus SUVr	-2.35(0.143)	0.189
	Anterior cingulate SUVr	-0.91(0.470)	0.174

Coeff. β: coefficient β, SUVr: Standardized Uptake Value ratio; MoCA: Montreal Cognitive Assessment; TMT: Trail Making Test; CVLT: California Verbal Learning Test –II; PCC: posterior cingulate cortex. (All coefficient β values are adjusted for the covariates age, sex and education. Adjusted R square is the proportion of variance in the cognitive function scores that was explained by the model discounted for age, sex, education and regional SUVr).

Figure 2.2 Scatterplot between the mean score of posterior cingulate cortex and precuneus SUVr with cognitive function scores (MoCA and TMT B-A)

Figure A   Figure B
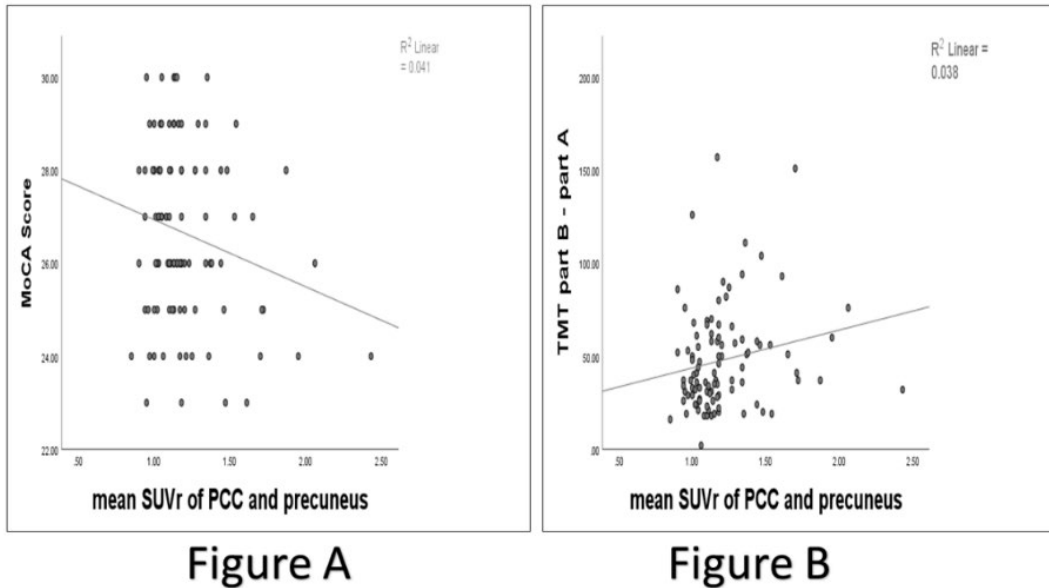
The scatterplots show the fitted regression line of the posterior cingulate cortex (PCC) and precuneus SUVrs as independent variables and cognitive function test scores (MoCA global score, and TMT part B completion time- TMT part A completion time) as the dependent variable. Figure A: Removing the visually obvious outlier (The mean SUVr of PCC and precuneus = 2.43 (p =0.048)) did not alter the statistical significant correlation between MoCA global score and the mean SUVr of PCC and precuneus.

2.4　Discussion

The main finding of this study is that regional amyloid deposition in the precuneus and posterior cingulate are associated with early preclinical decline in executive function in pAD, irrespective of global SUVr. Prior studies that have focused on regional amyloid deposition in the brain have shown that regional amyloid deposition in posterior cingulate gyri and precuneus are associated with global cognition [122, 123] and lower preclinical memory scores; however, analyses of Aβ influences on non-memory cognitive domains were not assessed [123-125]. Such studies with an *a priori* focus on memory domain impairment rather than exploring a broader array of cognitive domain relationships introduces a bias that limits our full understanding of the impact of early preclinical Aβ deposition.

While the majority of observational studies and clinical trials for pAD have defined populations on the basis of global SUVr cut-offs, the present data suggests that such criteria may be selecting for a later pathological stage of disease, perhaps mediated by cognitive reserve mechanisms. As the field moves towards earlier diagnosis and intervention, considering the development of modified biomarker criteria that takes into account the wealth of data accumulated in the area of pAD just makes sense. Such attempts to date, include lowering global Aβ SUVr cut-off scores for the diagnosis of pAD [126-128], that have enabled an even earlier examination of pAD. Our data suggests we can go even earlier by focusing on regional Aβ -PET SUVr levels in the precuneus and posterior cingulate rather than on global SUVr data that has already been adjusted to its threshold. While concerns about using such an approach might include a possibility of simply detecting incidental cerebral amyloidosis that may never progress, the present data demonstrating early preclinical cognitive test score associations argue against such a possibility, demonstrating that such early regional Aβ deposition is clinically meaningful. Moreover, accumulation of amyloid in precuneus had shown to be predictive of future global amyloid deposition in the brain [123].

In this context, the present data demonstrate that changes in executive function may be the earliest signs of pAD. Consistent with our findings, Snitz et al. reported that nonmemory domains, primarily executive functions is changed 7 to 9 years prior to neuroimaging change in Aβ-positive clinically normal participants comparing to Aβ-negative participants [50]. A more recent study using random forest machine learning analysis to rank the AD biomarkers in prediction of clinical dementia status in AD [129] found that Aβ deposition in precuneus, temporal and frontal as well as tau levels are highly correlated with cognitive function in

cognitively normal participants and are predictors for early preclinical impairments in executive and memory function. This same study also demonstrated that increased tau burden is associated with lower memory but not executive function scores in clinically normal older individuals. Our data is aligned with these previous results suggesting that early change in executive function in pAD may be explained by preclinical Aβ deposition in precuneus and posterior cingulate gyri. Both posterior cingulate gyri and precuneus are part of default mode network, which is involved in attention and executive function [130].

It is also possible that the lower executive function performance associated with early preclinical Aβ deposition in the precuneus and posterior cingulate seen in the present study may not be dependent on neuroanatomic involvement of these regions but rather may be associated with more global changes in brain function and or pathology that lie below the level of Aβ -PET detection. As such, it is possible that early Aβ deposition in the precuneus and posterior cingulate is related to a more widespread production of early synaptotoxic soluble oligomeric Aβ species affecting regions such as the dorsolateral prefrontal cortex that is more widely recognized as a neuroanatomic substrate for executive dysfunction [131]. Interstitial fluid accumulation of such soluble oligomeric Aβ species may be well below the threshold of Aβ -PET detection. Alternatively, early tau abnormalities, inflammatory, or oxidative stress related mechanisms are just a few of the concomitant mechanisms that could be at play but remain below the level of detection in brain regions responsible for early executive dysfunction in pAD [132]. Much further work is needed before we fully understand the still enigmatic state of pAD.

Cognitive screening instruments such as MoCA are widely used to detect cognitive decline as one transitions from pAD to mild cognitive impairment or dementia due to AD [43], but are relatively insensitive for tracking cognitive decline in pAD. Our data, however, using adjusted linear multiple regression, demonstrates that increased Aβ deposition in the precuneus and posterior cingulate (the earliest brain regions affected with Aβ pathology[3, 102]) are associated with decreased global cognitive performance MoCA, further supporting at least one prior study in the literature [133]. The relationship of MoCA scores with Aβ deposition in the precuneus and posterior cingulate seen in the present study appeared to be driven by language domain subscores in individuals with pAD (data not shown). This result conceptually is in accordance with prior findings from a much smaller study (n =11 AD and 15 healthy control) that found a significant relationship between greater florbetapir F18 precuneus SUVr and poorer verbal fluency in AD [134].

The main limitations of our study include the relatively small sample size, and an absence of tau measures in the analysis. Another main limitation of the study is unavailability of APOE in the analysis, despite its well-recognized influence on amyloid deposition in cognitively healthy individuals. Another limitation of this study is the use of a highly educated, predominantly white sample that limits the generalizability of the results to underrepresented groups. Despite this limitation it should be noted that the participants represented a well-characterized cohort that has undergone comprehensive longitudinal medical and neuropsychological exams. The strengths of our work include a focus on early regions of the brain affected by Aβ pathology and their relation to domain-specific cognitive test performance in pAD, prior to development of global Aβ positivity.

While the prevailing view in the field suggests that memory performance is the earliest clinical hallmark of AD, the present data demonstrate that changes in executive function, mediated by Aβ deposition in the precuneus and posterior cingulate may precede memory decline in pAD. Ongoing and future efforts at developing more sensitive tests for preclinical executive function deficits may serve as the most sensitive, low cost, non-invasive clinical biomarkers of preclinical AD. Further studies are needed to show the longitudinal clinical and cognitive outcome of this early preclinical amyloid change, and for a complete understanding of the temporal progression of domain specific cognitive change in relation to regional progression of amyloid deposition in the brain.

CHAPTER 3.   AMYLOID-PET AND WHITE MATTER HYPERINTENSITIES HAVE INDEPENDENT
EFFECTS ON BASELINE COGNITIVE FUNCTION AND SYNERGISTIC EFFECTS ON LONGITUDINAL
EXECUTIVE FUNCTION

3.1   INTRODUCTION

Alzheimer's disease (AD) and subcortical vascular dementia are considered the most common pathologic contributors to dementia in the aging population. Both frequently coexist in over 80% of community dwelling adults with dementia [135]. Cerebral small vessel disease (CSVD) has also been linked to the pathogenesis of AD and is largely responsible for the development of subcortical vascular dementia [61]. AD and CSVD share multiple risk factors [136], occurring concomitantly in over 50% of individuals with dementia [137], and there may be substantial overlap between these two conditions in terms of clinical, pathological and radiological findings. Co-occurrence of beta amyloid (Aβ) (a hallmark pathologic feature of AD) and white matter hyperintensities ((WMH), reflecting CSVD burden) increase the risk of dementia [74].

WMH and Aβ are also key drivers of cognitive decline in healthy older adults, and both are considered biomarkers of preclinical dementia [77, 138]. Neuroimaging studies examining the combined impact of Aβ burden and WMH on cognition have largely examined these variables independently rather than examining the potential interplay between these key pathologic hallmarks of dementia. Several studies have addressed this issue of interplay between Aβ and WMH with often contradictory results [59, 76, 77, 80, 81, 138-141]. Notably, many of these studies focused on global measures of WMH and Aβ without exploration of regional effects in relation to stage of disease. Studying the effect of Aβ and WMH on cognition without emphasizing the importance of lesion location can miss the functional consequences of the two pathologies. Previous studies investigating the impact of regional distribution of WMH on (executive function) EF found that WMH in all cortical regions (frontal areas, occipital, parietal and temporal) are associated with deficits in EF scores [97, 142, 143], but regional quantification of Aβ and its interaction with WMH volume has not been fully investigated in these prior studies.

Aβ deposition is hypothesized as being the initial step in the neuropathological development of AD and dementia [144], but findings from previous studies have also shown that WMH often occur prior to the presence of amyloid-β plaques in preclinical AD [145-147] supporting a retrograde degeneration hypothesis [148, 149]. Additionally, evidence from recent

studies has suggested that the relationship between WMH and Aβ is strongly determined by the spatial distribution of the two pathologies [150]. The majority of published studies have emphasized the spatial heterogeneity of WMH [98, 151], but have left the potential heterogeneous influences of regional Aβ deposition relatively unexplored.

Since mixed dementia is widely recognized as the norm rather than the exception, in the present study we sought to explore the relation between regional and global Aβ and WMH with cognitive function (EF and memory) scores in cognitively normal (CN) older adults at baseline, and further examine the relation between WMH and regional Aβ deposition in relation to cognitive performance changes over time.

3.2   Methods

Data used in the preparation of this article were obtained from the summary data from Alzheimer's Disease Neuroimaging Initiative (ADNI) database (adni.loni.usc.edu). The ADNI was launched in 2003 as a public-private partnership, led by Principal Investigator Michael W. Weiner, MD. The primary goal of ADNI has been to test whether serial magnetic resonance imaging (MRI), positron emission tomography (PET), other biological markers, and clinical and neuropsychological assessment can be combined to measure the progression of mild cognitive impairment (MCI) and early Alzheimer's disease (AD).

3.2.1   Participants:

Summary data from the Alzheimer's Disease Neuroimaging Initiative (ADNI 2) at http://adni.loni.usc.edu [152] were used in the present analyses. Only participants with a mini-mental state examination (MMSE) score greater than or equal to 26 at baseline meeting these inclusion criteria were included in the analysis: (1) Complete demographic information (i.e., age, sex, education) and ApoE genotype available; (2) Neurocognitive composite metrics for EF and memory at baseline and after approximately 2 years; (3) PET Florbetapir for focal and global Aβ quantification; and (4) T2 FLAIR scan acquisition with WMH volume quantification. Details of ADNI inclusion criteria, clinical procedures and methodology are available elsewhere [153, 154]. These criteria were developed to specifically investigate predisease and preclinical disease states that may lead to further cognitive impairment and dementia.

Participants with missing data required for the analyses were excluded. A total of 53 participants were excluded from the longitudinal analysis on the basis of missing data required for the analysis. Excluded participants did not differ significantly from these included in the analysis in regards to age, sex, education, ApoE, or baseline MMSE scores (data not shown).

3.2.2   Imaging analysis

3.2.2.1   White Matter Hyperintensity quantification method

WMH volumes were quantified using the 4-tissue segmentation method described previously [68]. Briefly, first step was co-registration of the FLAIR to the 3D T1 image inhomogeneity-corrected and non-linearly aligned to a minimal deformation template (MDT) using the T1 transformation and the FMRIB Software Library (FSL) toolbox[155, 156]. Modified Bayesian probability and structure prior probability maps were used to estimate WMH in the MDT. Binary WMH masks were then created using 3.5 SD threshold above the mean. The segmented WMH masks were then back-transformed into native space for tissue WMH volume calculation. An Expectation-Maximization (EM) algorithm was used for segmentation to isolate gray, white, and CSF measurements in template-space. Transforming these masks back to each image's native space produced rough estimate 3-tissue segmentations. Finally, WMHs were ultimately subtracted from segmented white matter volume and reported in cubic millimeters.

3.2.2.2   Calculation of Florbetapir cortical summary values.

Preprocessing of the AV-45 PET scans and computation of the global AV-45 PET values were done centrally by the ADNI core as described previously [157]. Briefly, each subject's florbetapir image was coregistered using SPM8 to that subject's MRI image that was closest in time to the florbetapir scan. Freesurfer processing was carried out to skull-strip, segment, and delineate cortical and subcortical regions in all MRI scans[158, 159]. Volume-weighted florbetapir means from a cortical summary region were extracted. A single binary cortical summary region composed of all the subregions was created to calculate the mean uptake across each region. We used the summary data of global and regional (frontal, parietal, and cingulate regions that have been most frequently associated with EF performance [51, 160-162]) SUVr determination was based on the whole cerebellum reference region. Details regarding regions of

interest forming the subregions frontal, parietal and cingulate have been described previously [157].

3.2.3 Composite measures of executive function and memory: ADNI_EF and ADNI_Memory

The specific tests included in ADNI executive function (ADNI-EF) composite scores are Category Fluency (animal &vegetable naming), Trail Making Tests A and B, Digit Span backwards, Wechsler adult intelligence scale-revised (WAIS-R) Digit Symbol Substitution, and 5 Clock Drawing items (circle, symbol, numbers, hands, time). The memory composite (ADNI_Memory) included the Rey auditory verbal learning test (RAVLT), the cognitive component of the Alzheimer's disease assessment scale (ADAS-Cog), and Wechsler logical memory scale scores [163]. We used the ADNI-EF and ADNI-Memory scores corresponding to the baseline scan and EF and memory scores within one to three years from the baseline as follow-up scores.

3.2.4 Statistical analyses:

All statistical analyses were conducted using SPSS, version 26.0 (SPSS Inc., Chicago, IL, USA). Significance was set at $P < .05$, with Bonferroni correction based on the number of the analysis. We used multiple regression models including the interaction term and the main effects for Aβ and WMH to investigate the independent and combined associations of these pathologies with cognition (ADNI-EF and ADNI-Memory). WMH volume was logarithmically transformed due to the positive skewed distribution for the statistical analysis. Moderation analyses assessing the relationship between Aβ and WMH were fit to the data using the following equation:

$$\hat{Y} = b_0 + b_1 WMH + b_2\, A\beta + b_3 WMH*A\beta + bX,$$

where $\hat{Y}$ represents the mean and bX represents beta coefficients and adjustment covariates. Age (continuous values), sex (indicator variable), education (continuous values), ApoE (indicator variable), and total intracranial volumes (continuous values) were entered as covariates in all analyses. The models were built using Hayes' PROCESS macro for SPSS (model 1) [164]. Longitudinal analyses examined the association of the interaction between baseline Aβ burden and WMH with mean follow-up cognitive (ADNI-EF or ADNI-Memory) scores after controlling for baseline ADNI cognitive scores and time following the baseline scan acquisitions and cognitive testing. To consider the regional Aβ burden effects in addition to global Aβ burden and

WMHs on baseline and change in ADNI-EF and ADNI-Memory, moderated regressions were run for amyloid deposition (SUVr) in each of the *a priori* selected cortical regions (Frontal, cingulate and parietal), adjusting for age, sex, education, ApoE, and intracranial volumes.

Assuming that WMH is causally related to Aβ deposition, which is in turn causally related to cognitive (ADNI-EF or ADNI-Memory) scores, mediation models were built to estimate the relationship between WMH (independent variable) and cognitive function (dependent variable) and Aβ (mediator variable). This model was built using Hayes' PROCESS macro for SPSS (model 4) [164]. Significance was tested using 5000 bootstrap samples to calculate bias-corrected 95% confidence intervals. Indirect effects with bootstrapped 95% confidence intervals not crossing zero were considered significant. Age, sex, education, ApoE, and intracranial volumes were entered as covariates in the mediation regression models. Baseline ADNI composite scores and times between the two cognitive scores tests were added as covariates in the mediation regression models examining longitudinal cognitive score changes.

3.3   Results

The demographic, clinical and imaging characteristics of the included participants are provided in Table 3.1. Briefly, the sample included 326 women and 388 men with a mean age of 73.13±7.4 years; participants were highly educated on average (16.3±2.6 years).

Table 3.1 Characteristics of participants

Characteristic	Range	Mean (SD)	Sample size
Age (years)	55-96	73.13 (7.41)	714
Education (years)	10-20	16.31 (2.6)	714
Global Aβ burden (SUVr)	0.84 – 2.01	1.19 (0.22)	714
Frontal Aβ burden (SUVr)	0.83 -2.01	1.19 (0.23)	714
Cingulate Aβ burden (SUVr)	0.89 – 2.36	1.29 (0.22)	714
Parietal Aβ burden (SUVr)	0.87 – 2.08	1.20 (0.22)	714
WMH volumes in cubic centimeters	0.07 - 61.02	6.94 (8.54)	714
WMH volume (log-transformed)	-1.13 to 1.79	0.57 (0.52)	714
Total intracranial volumes	1084.29 to 1861.82	411.88 (135.97)	714
ADNI-EF (baseline)	-3.01 to 2.99	0.54 (0.94)	714
ADNI-EF (follow-up)	-3.01 to 2.99	0.50 (1.06)	661
ADNI-memory (baseline)	-2.8 to 3.14	0.56 (0.81)	714
ADNI-memory (follow-up)	-2.62 to 3.06	0.52 (0.94)	661
Time between test (years)	1 to 3	1.86 (0.49)	661
APOE e4 allele N(%) copy1	2 to 4	58 (8.1)	714
APOE e4 allele N(%) copy 2	3 to 4	300 (42.1)	714
Sex male N (%)		388 (54.3)	714

Key: Aβ, Beta Amyloid; WMH, White Matter Hyperintensities; ADNI-EF, Executive Function; SD, Standard Deviation; SUVr, Standardized Uptake Value Ratio.

3.3.1 Testing the interaction term and the main effect of global, and regional Aβ burden and WMHs with cognition

The moderation regression analysis detected a marginally statistically significant interaction effect between Aβ burden and WMH in relation to baseline EF (p-value=0.061), and a significant interaction term between the biomarkers in relation to longitudinal executive functions

with p-value= 0.036. Overall, when amyloid burden was higher, the association between log WMH and ADNI-EF was stronger. (+1SD above sample mean) (Figure 3.1A). Regarding memory composite scores, the models did not detect any statistically significant interaction effect between global Aβ burden and WMH in relation to baseline ADNI-memory scores or follow-up ADNI-memory scores (p-value 0.401 and 0.937 respectively).

The regional models examining the interaction between Aβ burden in discrete cortical regions and WMH volumes detected marginally significant interaction between frontal, parietal, and cingulate Aβ burden and WMHs in relation to baseline EF performance with p values (0.061, 0.059, and 0.071) respectively. In contrast, the models failed to detect even marginally significant interaction effects between regional Aβ burden and WMHs with baseline memory (p-values for interaction term were in frontal Aβ 0.360, parietal Aβ 0.353, and cingulate Aβ 0.411).

The moderation analysis detected a significant interaction effect of frontal and cingulate Aβ burden and WMH on longitudinal EF performance with p value 0.033 for frontal and 0.024 for cingulate (Figure 3.1B and 3.1C). The (regression) slopes illustrating the negative association of WMH volume with longitudinal executive function performance for 3 levels of regional Aβ burden and WMHs (−1, 0 and 1 SD using sample's mean) are shown in Figure 3.1. In contrast to the results for EF, the moderation regression analysis failed to detect a statistically significant interaction effect between regional Aβ burden and WMH in relation to follow-up ADNI-memory scores. Results regarding the moderation models between global and regional Aβ burden and WMH with baseline and follow-up cognitive (ADNI-EF and ADNI-Mem) scores are displayed in supplementary tables 3.2 and 3.3.

Table 3.2: The interaction between global and regional Aβ burden and WMHs on cross-section and longitudinal performance in EF

	Baseline EF		Longitudinal EF	
	Coefficient	P value	Coefficient	P value
Main effect of WMH	-0.198	0.003*	-0.073	0.177
Main effect of Global SUVr	-1.162	<0.001**	-0.708	<0.001**
Interaction WMH * Global SUVr	0.517	0.061	-0.482	0.029*
Main effect of WMH	-0.203	0.003*	-0.094	0.097
Main effect of Frontal SUVr	-1.104	<0.001**	-0.672	<0.001**
Interaction between WMH * Frontal SUVr	0.496	0.061	-0.452	0.033*
Main effect of WMH	-0.185	0.006*	-0.086	0.112
Main effect of Parietal SUVr	-1.126	<0.001**	-0.701	<0.001**
Interaction between WMH * parietal SUVr	0.505	0.059	-0382	0.052
Main effect of WMH	-0.217	0.015*	-0.098	0.144
Main effect of Cingulate SUVr	-0.801	<0.001**	-0.678	<0.001**
Interaction between WMH *cingulate SUVr	0.488	0.071	-0.455	0.024*

Key: WMH, white matter hyperintensities; EF, Executive function; SUVr, standardized uptake value ratio; ** less than 0.001, * less than 0.05

Table 3.3 The interaction term and the main effect of global, and regional Aβ burden and WMHs with memory score:

	Baseline ADNI-Memory score		Follow-up ADNI-Memory score	
	Coefficient	P_value	coefficient	P_value
Main effect of WMH	-0.0753	0.202	-0.108	0.004
Main effect of Global SUVr	-1.257	<0.001**	-0.439	<0.001**
Interaction between WMH * Global SUVr	0.196	0.401	-0.012	0.937
Main effect of WMH	-0.078	0.170	-0.109	0.003*
Main effect of Frontal SUVr	-1.189	<0.001**	-0.491	<0.001**
Interaction between WMH * frontal SUVr	0.205	0.360	-0.051	0.917
Main effect of WMH	-0.063	0.291	-0.105	0.005*
Main effect of Parietal SUVr	-1.179	<0.0001**	-0.405	<0.001**
Interaction between WMH * parietal SUVr	0.209	0.353	0.021	0.887
Main effect of WMH	-0.079	0.119	-0.113	0.003*
Main effect of Cingulate SUVr	-1.015	<0.001**	-0.369	<0.001**
Interaction between WMH *cingulate SUVr	0.188	0.411	-0.007	0.923
Main effect of WMH	-0.083	0.14	-0.112	0.003*
Main effect of temporal SUVr	-1.366	<0.001**	-0.464	<0.001**
Interaction between WMH*Temporal SUVr	0.208	0.406	-0.026	0.873

Key: WMH, white matter hyperintensities; EF, Executive function; SUVr, standardized uptake value ratio; ** less than 0.001, * less than 0.05

Figure 3.1   Longitudinal EF performance at low (−1 SD), moderate (mean (0 SD), and high (1 SD) levels of baseline global and regional Aβ burden and WMH
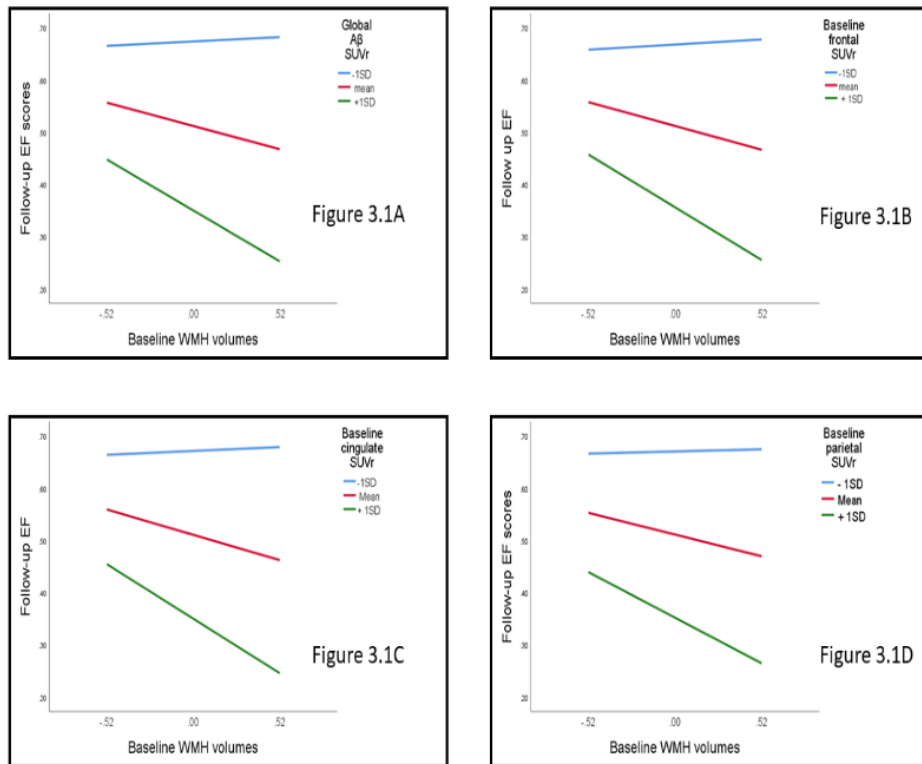
The (regression) slopes representing WMH's negative associations with executive functions for high levels of regional Aβ burden (+1 SD using sample's mean). Figure 3.1A showed the interaction term of global Aβ burden and WMHs with Follow-up ADNI-EF scores. Overall, when amyloid burden was higher, the association between log WMH and ADNI-EF was stronger. (+1SD above sample mean). Figure 3.1B showed the interaction term of frontal Aβ burden and WMHs with Follow-up ADNI-EF scores. Figure 3.1C showed the interaction term of baseline cingulate Aβ burden and WMHs with Follow-up ADNI-EF scores. Figure 3.1D showed the interaction term of baseline parietal Aβ burden and WMHs with Follow-up ADNI-EF scores.

3.3.2   Testing the mediation effects of global and regional Aβ burden on WMH related cognitive performance

Mediation analyses were conducted to assess whether global and regional Aβ burden act as potential mediators of the relationship between WMH and cognitive performance. Path models of the mediation effect are presented in Figures 3.2, 3.3, 3.4 and 3.5. The path analysis revealed that global Aβ deposition mediates the relationship between WMH and baseline cognitive (EF and memory) scores (see figures 3.2A, 3.3A). The bootstrap confidence interval (CI) for the indirect effect demonstrated that the indirect effect of WMH on baseline EF performance (a× b = −0.045;

CI: −0.09, −0.01) and baseline memory scores (CI: −0.01, -0.006) through global Aβ burden were significant. Both Frontal and parietal Aβ SUVr mediated the effect of WMH on baseline EF and memory performance (see figure 3.2B, 3.2D, 3.3B, and 3.3D). In contrast, there was no significant mediation effect by cingulate Aβ SUVr for baseline cognitive performance (see figures 3.2C and 3.3C). The other model explored whether global and regional Aβ SUVr mediated the relationship between WMH and follow-up cognitive (EF and memory) scores after adding baseline cognitive scores and times since the initial cognitive test as the covariates. Results demonstrated that neither global Aβ SUVr nor regional Aβ SUVr mediates these associations as the CI for the indirect effect was crossing the zero and did not reach statistical significance (see figure 3.4 and 3.5). While our path analyses were conducted to assess whether global and regional Aβ burden act as potential mediators of the relationship between WMH and ADNI-memory scores, we tested its opposite direction, and no significant mediating effects were detected for baseline and follow-up ADNI-memory scores. (See supplementary figures 3.6 and 3.7)

Figure 3.2 Path models of the mediation effect of global and regional Aβ burden between WMH and baseline EF performance
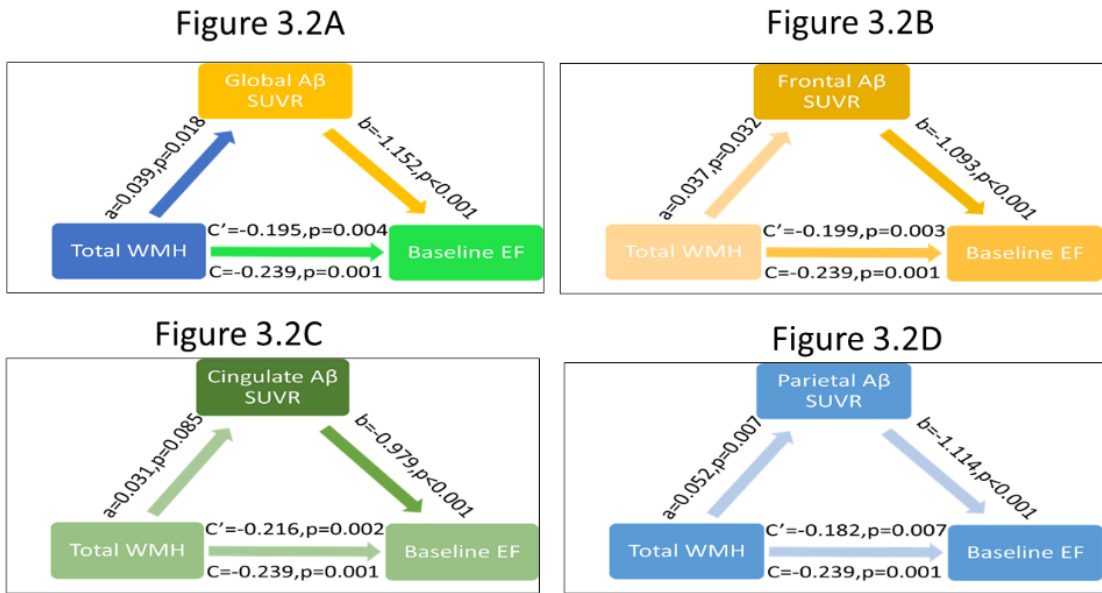
As such, path a is expressed the change in Aβ SUVr with one unit increase in WMH, whereas path b is expressed decrement of baseline EF associated with an increment of Aβ SUVr. Path c' the direct effect of WMH on EF and path c (total effect). The confidence intervals for the indirect mediation effects of WMH on baseline EF through frontal Aβ (a× b = −0.045; CI: −0.08, −0.005) and parietal Aβ (a× b = −0.058; −0.11, −0.02) were significant. (WMH, white matter hyperintensities; EF, Executive function; SUVr, standard uptake value ratio; Aβ, beta amyloid)

Figure 3.3 Path models of the mediation effect of global and regional Aβ burden between WMH and baseline ADNI-memory scores
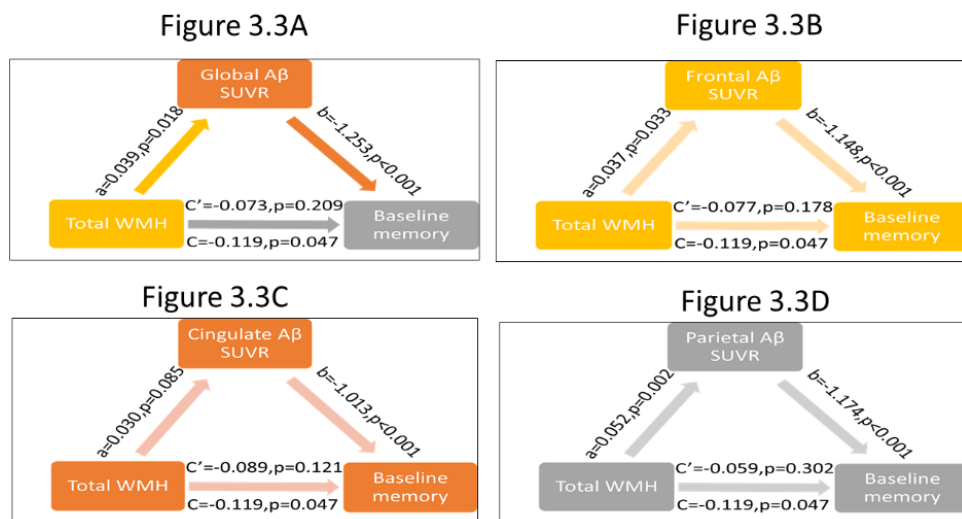
As such, path a is expressed the change in Aβ SUVr with one unit increase in WMH, whereas path b is expressed decrement of baseline ADNI-memory scores associated with an increment of Aβ SUVr. Path c' the direct effect of WMH on ADNI-memory scores and path c (total effect). The confidence intervals (CI) for the indirect mediation effects of WMH on baseline ADNI-memory scores through global (CI: −0.01, -0.006), frontal Aβ (CI: −0.11, -0.01), cingulate Aβ (CI: −0.07, 0.004), and parietal Aβ (CI: −0.11, -0.02). (WMH, white matter hyperintensities; SUVr, standard uptake value ratio; Aβ, beta amyloid; CI, confidence intervals).

Figure 3.4 Path models of the mediation effect of baseline global and regional Aβ burden on longitudinal EF performance
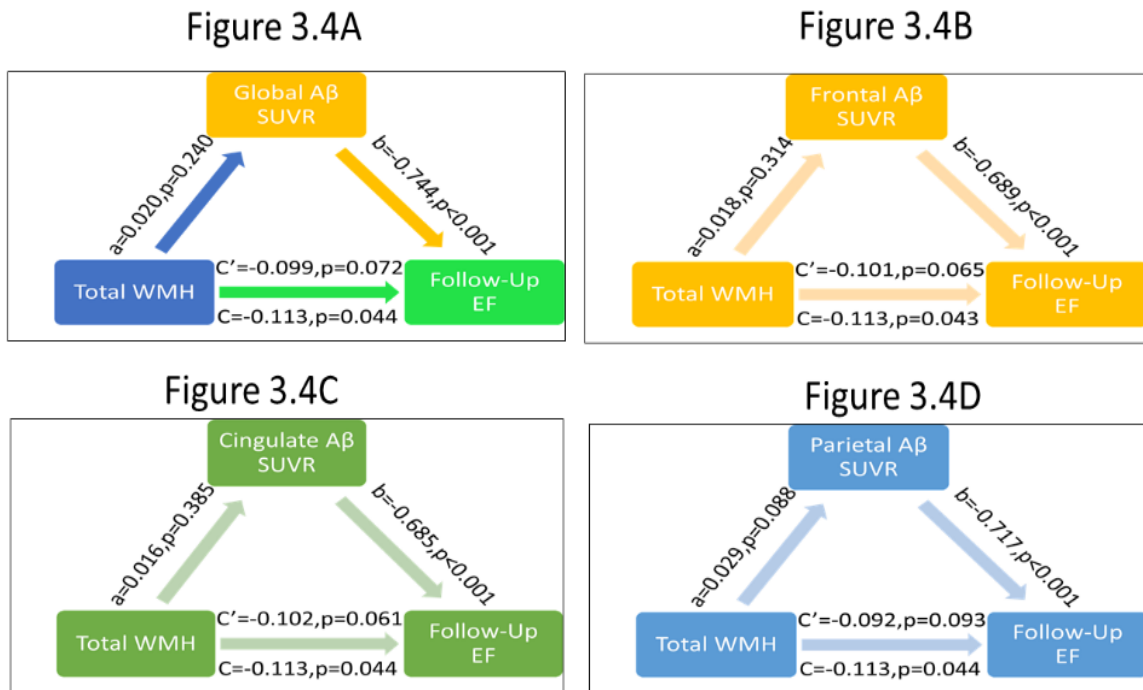
As such, path a is expressed one unit increase in WMH associated with increase of Aβ SUVr , whereas path b is expressed the change in longitudinal EF associated with an increment of Aβ SUVr. Path c' the direct effect of WMH on EF and path c (total effect). The confidence intervals (CI) for the indirect mediation effects of WMH on follow-up EF scores through global Aβ SUVr ((a× b = −0.015; CI :−0.045, 0.009), frontal Aβ (a× b = −0.012; CI: −0.041, 0.011), cingulate Aβ (a× b = −0.011; CI: −0.04, 0.014), and parietal Aβ (a× b = −0.021; CI: −0.05, 0.01). (WMH, white matter hyperintensities; EF, Executive function; SUVr, standard uptake value ratio; Aβ, beta amyloid; CI, confidence intervals)

Figure 3.5 Path models of the mediation effect of baseline global and regional Aβ burden on longitudinal memory performance
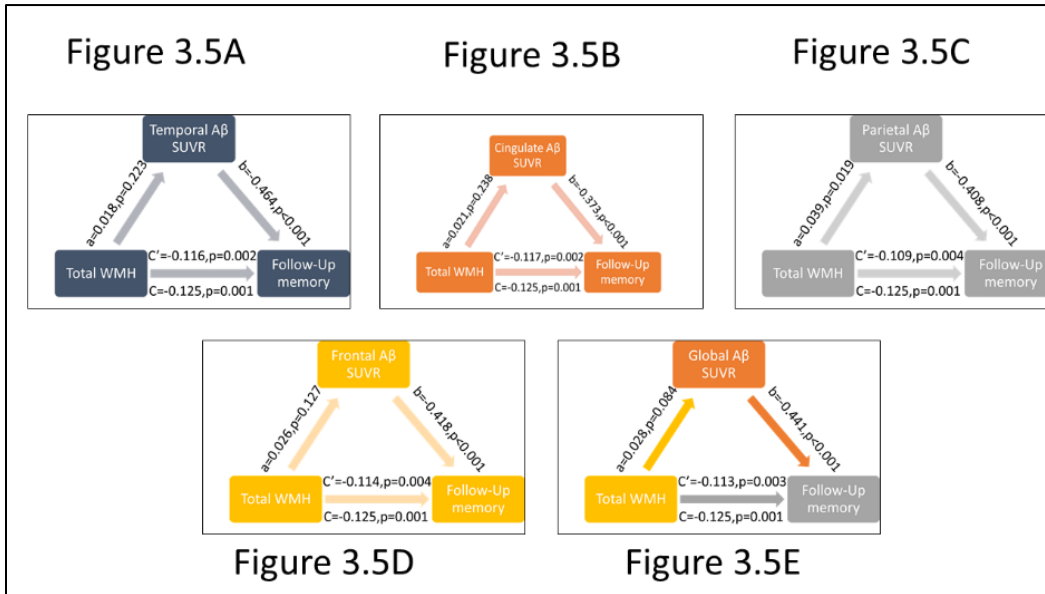
As such, path a is expressed one unit increase in WMH associated with increase of Aβ SUVr, whereas path b is expressed the change in follow-up ADNI-memory scores associated with an increment of Aβ SUVr. Path c' the direct effect of WMH on follow-up ADNI-memory scores and path c (total effect). The confidence intervals (CI) for the indirect mediation effects of WMH on follow-up ADNI-memory scores through temporal Aβ (CI:-0.026, 0.06) cingulate Aβ (CI: −0.024, 0.05), parietal Aβ (CI: −0.035, 0.002), frontal Aβ (CI: −0.028, 0.04), and global Aβ (CI: −0.031, 0.002) were crossing zero. (WMH, white matter hyperintensities; SUVr, standard uptake value ratio; Aβ, beta amyloid; CI, confidence intervals).

Figure 3.6 path models of the mediation effect of WMH between global and regional Aβ burden and baseline ADNI-memory scores
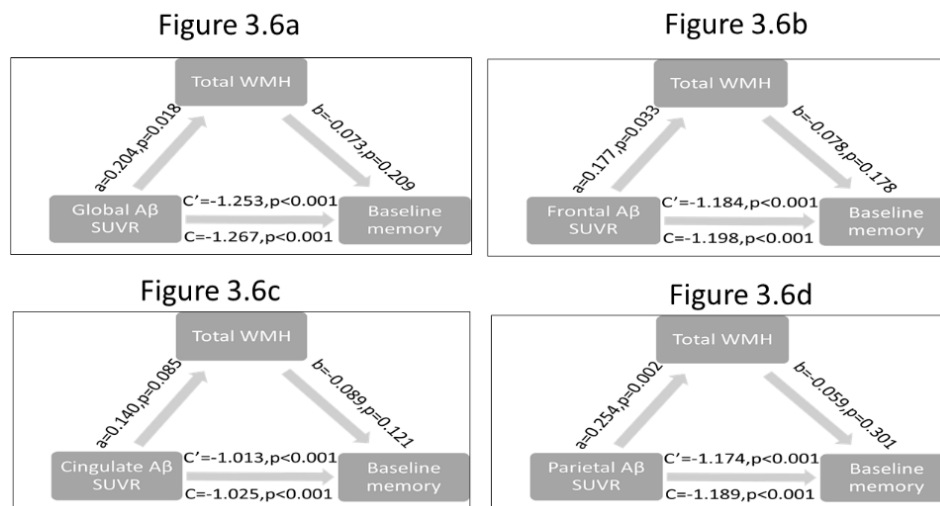
As such, path a is expressed the change in WMH volumes with one unit increase in Aβ SUVr, whereas path b is expressed decrement of baseline ADNI-memory scores associated with an increment of WMH. Path c'

the direct effect of Aβ SUVr on ADNI-memory scores and path c (total effect). The confidence intervals (CI) for the indirect mediation effects of WMH on baseline ADNI-memory scores through global (CI: −0.043, 0.007), frontal Aβ (CI: −0.039, 0.05), cingulate Aβ (CI: −0.039, 0.04), and parietal Aβ (CI: −0.046, 0.012) were crossing zero indicating no significant mediating effects.

Figure 3.7 path models of the mediation effect of baseline WMH volumes on follow-up ADNI-memory performance

Figure 3.7a

Figure 3.7b

Figure 3.7c

Figure 3.7d

Figure 3.7e
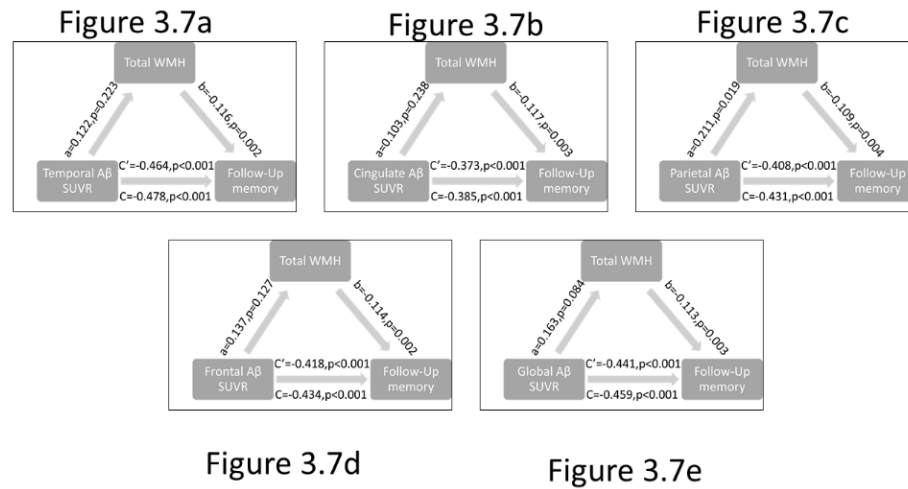
As such, path (a) is expressed one unit increase in Aβ SUVr associated with increase of WMH volumes, whereas path (b) is expressed the change in follow-up ADNI-memory scores associated with an increase in WMH volumes. (Path c') the direct effect of Aβ SUVr on follow-up ADNI-memory scores and path c (total effect). The confidence intervals (CI) for the indirect mediation effects of WMH on follow-up ADNI-memory scores through temporal Aβ (CI:-0.04, 0.01) cingulate Aβ (CI: −0.036, 0.009), parietal Aβ (CI: −0.052, 0.0001), frontal Aβ (CI: −0.024, 0.006), and global Aβ (CI: −0.047, 0.04) were crossing zero indicating no significant mediating effects.

3.4 Discussion

The present results indicate that there is an independent effect of both Aβ and WMH on cognitive performance at baseline and a synergistic interaction between these baseline biomarkers of pathology on longitudinal EF performance. This synergistic effect was not seen in longitudinal memory performance. The other main finding, demonstrated through mediation analysis, is that the extent of WMH dependent changes in baseline EF was mediated by both global and regional Aβ burden. Thus, WMH accumulation appears to increase Aβ deposition which in turn influences cognition longitudinally.

The present moderation analysis provides evidence of an additive effect of WMH and Aβ in relation to baseline cognitive performance, which is consistent with the findings from other

cross-section biomarker studies [59, 76-78]. The present study extends the results from previous studies by analyzing the effect of baseline biomarkers of Aβ and WMH on longitudinal cognitive performance. The data demonstrate that the combined effect of Aβ burden and WMH on longitudinal EF is greater than the sum of the two individual biomarker effects supporting a hypothesis of synergistic interactions between both Aβ and WMH. The synergistic effect between the baseline biomarkers of pathology on longitudinal EF performance was not seen in longitudinal memory performance. This finding may be related to the population studied as ADNI participants are largely well-educated and ADNI excludes participants with severe CSVD. One previous study showed that CN participants with low WMH volumes underwent low to no changes in memory performance, independent of amyloid burden [140]. Additionally, findings from another study have demonstrated that the association between WMH volumes and both EF and memory function were significant in demented participants but that the relationship between memory and WMH was not detected in CN participants, such as those included in the present study [165]. It is also possible that the synergistic effect seen in longitudinal EF performance but not memory performance may involve alterations in brain function and structure networks [166], WMH burden and/or Aβ deposition that were not included in the present analysis.

The present data further demonstrates that regional Aβ burden in frontal, and cingulate regions, are most related to WMH effects on longitudinal EF change. These data suggests that this relation might be explained by WMH impacts on connectivity within the executive control, and default mode networks [166]. Indeed, the present findings support the hypothesis that executive function performance is dependent on both intact white matter pathway connectivity, as well as pathologic integrity of the cortical regions themselves [141, 167, 168] and that there is a synergistic interaction between baseline biomarkers of pathology on longitudinal cognitive functions that is dependent on frontal-subcortical circuitry in cognitive aging and pAD [81].

Studying the independent associations of WMH and Aβ burden with baseline and longitudinal cognitive performance, the present data demonstrate that baseline EF performance is explained by both global amyloid burden and WMH, but that Aβ burden was the only predictor of longitudinal EF performance and baseline memory performance (See supplementary tables 3.2 and 3.3). Consistent with our findings, one recent study from the University of California, Davis Alzheimer's Disease Research Center (UCD ADRC) diversity cohort found that WMH were related to baseline EF, but not longitudinal change in EF [140]. Conversely, the same group has argued that baseline WMH likely represents only a small percentage of the final WMH [169],

suggesting that longitudinal EF performance may be most related to progression of WMH, rather than solely associated with baseline WMH. It is also possible that these findings are related to population studied, as ADNI excludes participants with severe vascular risk factors that may limit analysis of the full impact of WMH and other cerebrovascular injury in this cohort [76, 170]. It should also be pointed out that baseline WMH was one of the predictors for follow-up memory performance with Aβ burden. These findings emphasize the important role of WMH as a risk factor for future memory decline even if it may not affect baseline memory performance at the stage of pAD [140, 171].

The present data clearly demonstrate that WMHs contribute to global and regional Aβ burden pathology, exerting an effect on baseline cognitive performance through multiple pathways. Consistent with our findings, a recently published study based on the C6 project in the Medical Imaging Trial Network of Canada (MITNEC-C6), which differs from ADNI in being a WMH enriched cohort [172] demonstrated that the relation between global WMH and cognition was mediated by global Aβ burden and cortical atrophy. The authors interpreted their results to suggest that Aβ burden appears to be aggravated in participants with WMH supporting a synergistic pathophysiological process. They further hypothesized that the relationship between WMH and Aβ burden may be related to impaired general cerebral perfusion [74, 173] or to vascular pathology affecting amyloid clearance pathways [139]. Another possible explanation presented by the authors focused on myelin damage [174], which has been shown to promote Aβ oligomerization, eventually contributing to amyloid deposition [175]. These potential mechanisms may help explain the topographic patterns of regional Aβ deposition in relation to WMH effects on critical brain networks seen in the present study. The hypothesis of a regional association between Aβ and WMH is supported by the present data

One major limitation of the present study is the possibility of selection bias as ADNI excludes participants with significant evidence for cerebrovascular disease, which may limit discoveries into the interactions between Aβ and WMH that may exist in more generalizable samples. Further studies examining the interaction between Aβ and WMH in participants with higher levels of CSVD including lacunes, small subcortical infarctions, microinfarcts, and microbleeds are needed to fully investigate the associations of Aβ with CSVD. Additionally, the sample of participants evaluated is relatively small for moderation analyses but was restricted by the availability of extant data. Longitudinal outcome analyses may also be limited by the relatively short follow-up period in the ADNI 2 participants studied. It is possible that a more

extended follow-up period would help to clarify further the relationships between Aβ and WMH across progressive stages of cognitive decline, including MCI and early dementia stages.

Strengths of the present study include the use of ADNI data allowing analysis in a large sample of relatively homogeneous CN participants that have been classified extensively for the presence of pAD and CSVD. An additional strength is the use of both mediation and moderation analyses in studying the relation between cognitive function and the effects of the two primary drivers of dementia in the population (Aβ and WMH) within discrete brain regions. While to what extent WMH affects Aβ burden and cognition remain unclear, the present data demonstrate that baseline Aβ burden and WMH volumes have both independent associations with EF and memory scores at baseline, as well as synergistic associations with longitudinal EF performance. The extent of WMH dependent changes in baseline cognitive performance was related to both the direct effect of WMH and an indirect effect moderated through global and regional Aβ burden. The biological relationships between regional Aβ and WMH responsible for this indirect effect need further investigation across a broader profile of the disease course of dementia.

CHAPTER 4.   WHITE MATTER HYPERINTENSITIES INFLUENCE DISTAL CORTICAL b-AMYLOID ACCUMULATION IN DEFAULTS MODE NETWORK PATHWAYS

4.1   Introduction

Alzheimer's disease (AD) pathology can be influenced by modifying factors including age, APOE genotype and cerebral small vessel disease (SVD) among others [176, 177]. Despite findings from epidemiological and clinical-pathological studies supporting the relationship between SVD and AD [96, 147, 178-181], the mechanistic role of SVD in potentially contributing to the development and progression of AD pathology remains unclear [61]. To explore the effects of cerebral SVD on the development of AD, and vice-versa, studies that evaluate the pathological interplay between Aβ plaque deposition and White Matter (WM) alterations are needed. Findings from previous studies have demonstrated that WM alterations including white matter hyperintensities (WMH) often occur prior to the overt detection of amyloid-β deposition in preclinical AD (pAD) [145, 146, 182, 183]. Such findings support a hypothesis of retrograde degeneration, wherein axonal injury distal to the neuronal cell body, might upregulate amyloid production in connected cortical regions initiating and or accelerating the pathogenesis of AD.

Previous studies examining the relationship between WMH and AD pathology have shown that higher global WMH volume is associated with prefrontal and posterior cingulate Aβ deposition [184]. Increased global Aβ (measured in PET or CSF) has also been shown to be associated with posterior subcortical and periventricular WMH [97, 98, 185]. The main limitation of these studies involves the common use of global and or regional measures of WMH volume and Aβ deposition, rather than restricting the analyses to WMH in discrete fiber tracts and the upstream cortical regions where Aβ deposition occurs.

Recent studies on brain connectivity and functional neuroanatomy have enabled a better understanding of the potential mechanisms through which WM lesions may contribute to cognitive symptoms through disruption of the structurally connected cortical regions that represent the major networks of the brain [186, 187]. Moreover, WMH are associated with neuroinflammation that has been postulated to spread trans-axonally to interconnected cortical regions [188-190]. Among these networks, the default mode network (DMN) [191] plays a critical role in internally directed cognitive function. The DMN has been shown to exhibit not only functional disconnection, but also structural disruption associated with WM microstructural

disconnection associated with CSF Aβ levels [66, 192] or by WMH that are associated with cortical Aβ accumulation [193]. However, the association between WMH volumes specifically within DMN tracts, in relation to Aβ deposition in interconnected DMN cortical regions, has not been closely investigated. We specifically chose to focus on the DMN rather than other brain networks since it is affected in both AD and SVD [96, 194-197], suggesting it may be a good candidate network to explore in order to inform further understanding of the potential biological association between two pathologies. The main objective of this study was to test the hypothesis that WMH associated with Aβ levels within areas of the DMN that are disconnected by SVD early in the pathogenesis of AD in cognitively normal older adults with early Aβ deposition pAD. We aimed to evaluate Aβ SUVr in the cortical regions containing the neuron cell bodies of the DMN in relation to downstream WMH in interconnected axon tracts in the DMN.

4.2   Methods

4.2.1   Participants

72 subjects with normal cognition (mini-mental state examination (MMSE) score greater than or equal to 26) were identified in the multicenter network Alzheimer's Disease Neuroimaging Initiative (ADNI) at http://adni.loni.usc.edu, recruitment phase 3 by the following criteria: Complete demographic information (i.e., age, sex, education) and ApoE genotype, available availability of an AV-45 PET scan (to assess levels of Aβ), three-dimensional (3D) T1-weighted magnetic resonance imaging (MRI) scan (for spatial normalization and cortical parcellation), and 3D FLAIR scan (to assess WMH). Only subjects from ADNI 3 were included as previous ADNI cohorts did not include 3D FLAIR acquisitions required for precise WMH localization in DMN fiber tract pathways. Unfortunately, due to COVID interference with ADNI 3 recruitment and image acquisition, only a small cohort was available for the present analysis. Of note, we used all participants with available data at the time of this analysis. Details of ADNI inclusion criteria, clinical procedures and methodology are available elsewhere [153, 154]. A total of 8 participants were excluded from the analysis on the basis of missing data required for the analysis. Excluded participants did not differ from those included in the analysis in regards to age, sex, ApoE, or MMSE scores (data not shown).

4.2.2 Acquisition of florbetapir and MRI images

The MPRAGE sequence parameters included a Repetition time (TR) = 2300ms, Echo time (TE) = 2.26ms, inversion time (TI) = 900 ms, spatial resolution of $1 \times 1 \times 1 mm^3$. The 3D FLAIR sequence included a TR = 4800 ms, TE = 119 ms, TI = 1650 ms, spatial resolution of $1.2 \times 1 \times 1$ -mm^3 voxel resolution. AV-45 PET scans were acquired on a variety of different PET scanners (Siemens, GE and Philips) harmonized for ADNI data collection. AV-45 PET scans consisted of 4×300-second frames measured 50 minutes after injection of 10 ± 1.0 mCi of ^{18}F-Florbetapir AV-45

4.2.3 Florbetapir Amyloid PET processing and calculation of SUVr

Each participant's MPRAGE image was registered to the FLAIR images using FSL's linear registration tool (FLIRT) [198], then parcellated with FreeSurfer (v6.0) to derive cortical regions of interest for PET quantification.[158, 159] Pre-processed Florbetapir images were co-registered to the FreeSurfer-parcellated T1 image which was closest in time, using FreeSurfer's function *mri_coreg* as implemented in PETSurfer[199, 200]. Results were visually inspected to ensure correct co-registration. DMN regional amyloid burden was calculated using SUVr in the ADNI cortical summary region normalized by the whole cerebellum reference region.

4.2.4 Atlas-based fiber tract connecting DMN

We analyzed WMH volumes within major fiber tracts projecting from DMN regions using the Johns Hopkins University International Consortium for Brain Mapping probabilistic fiber tract atlas (JHU DTI-based white-matter atlases) [201]. The core DMN regions analyzed included the medial prefrontal cortex (MPFC), posterior cingulate (PCC), inferior parietal lobules (IPLs), and medial temporal lobe (MTL)[202]. The fiber tracts connecting the DMN cortical regions included the cingulum (CING) from PCC [203], cingulum–hippocampus tract (CING-Hippo) from MTL [203-205], superior longitudinal fasciculus (SLF) from IPL [206], and the inferior fronto-occipital fasciculus (IFOF) from MPFC [75, 100, 196, 207-211]. **(Table 4.1)**

Table 4.1 A description of the atlas-based fiber tracts connecting cortical regions in the DMN

DMN regions	JHU DTI-based white-matter atlases [201]	Freesurfer parcellation
MTL[203-205]	CING-Hippo	Entorhinal, Parahippocampal
MPFC[207, 208]	IFOF	Rostral Anterior cingulate, Caudal Anterior cingulate & Medial Orbitofrontal
PCC[203]	cingulum	Posterior cingulate
IPL[206]	SLF	Inferior Parietal

4.2.5   MRI analysis

4.2.5.1   WMH segmentation

3D FLAIR images were used to quantify WMH volume using semi-automated process that was developed in our lab as previously described [69, 70]. Briefly, 3D MPRAGE was co-registered to the FLAIR image using linear six parametric rigid body registration (FSL software library v5.0.8). The Brain Extraction Tool (BET), (http://fsl.fmrib.ox.ac.uk/fsl/fslwiki/BET), was used for non-brain tissue stripping of FLAIR images and to generate a binary brain mask. The binary brain mask was multiplied by the MPRAGE image to remove the non-brain tissue voxels. Statistical Parametric Mapping (SPM12) tool is operated based on MATLAB software (http://www.fil.ion.ucl.ac.uk/spm/), and was used for Multimodal segmentation to create separate native-space images representing gray matter (GM), white matter (WM), and cerebrospinal fluid (CSF) using an in-house segmentation validated template created from 145 images of healthy older adults [72]. WM was modeled as two separate tissue classes to capture all WM intensities. The two WM segmentation images were summed and convert to a binary WM mask in the native space. The WM binary mask was multiplied by the FLAIR image to generate WM image that is

mixed of normal appearing WM and WMH voxels. Gaussian fit was performed to the histogram of WM voxels was used to set the threshold for WMH as the mean plus $3 \times$ SD, corresponding to a P value of .01. Manual editing was required to remove false positive and artifact voxels from the total WMH mask. The total volume of the WMH voxel was the sum of all WMH mask voxels [69, 70].

4.2.5.2   Tract-related WMH volume

Each participant's MPRAGE image was registered to their FLAIR image using FSL's linear registration tool (FLIRT) [198], then registered to the MNI152 T1 template using FSL's non-linear registration tool (FNIRT) with standard parameters to generate the transformation matrix. Using the inverse transformation matrix and inverse non-linear warping parameters, JHU-ICBM-tracts atlas in MNI152 space [201] was then registered back to each participant's native space, effectively aligning it with their FLAIR image in the native space. Total WMH volumes in each tract were calculated by multiplying the registered binary tract to the WMH mask to derive the WMH volume within each specific fiber tract (Figure 4.1).

Figure 4.1 Diagram of the tract-related WMH volume quantification protocol
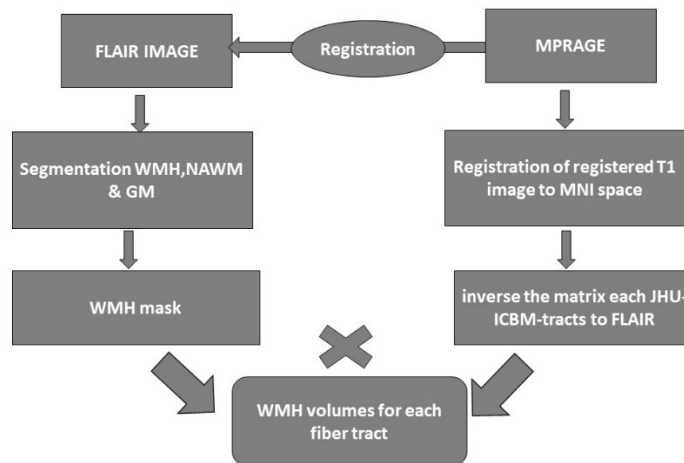
4.2.6 Statistical analysis

Statistical analyses were conducted using SPSS, version 26.0 (SPSS, Inc.). Significance was set at $P < .05$. To validate the relationship between regional Aβ and WMH burden, we used regression analysis between SUVr within gray matter of DMN regions as the dependent variable and WMH volumes within fiber tracts as independent variables. The general linear model was adjusted for the covariates age, sex, ApoE and total intracranial volumes. WMH volume within each fiber tract was logarithmically transformed due to the positive skewed distribution for the statistical analysis. The regression analyses assessing the relationship between Aβ and WMH were fit to the data using the following equation:

PET SUVr gray matter of DMN $= b_0 + b_1$ WMH volume (log-transformed) in JHU DTI-based white-matter atlases $+ \mathbf{bX}$, where $\mathbf{bX}$ represents beta coefficients and adjustment covariates.

4.3 Results:

The demographic and imaging characteristics of the sample are provided in table 4.2. Briefly, the sample included 33 women and 31 men with a mean age of 75.7±7.2 years.

Table 4.2 Demographic, clinical, imaging, and genetic characteristics of the cohort studied

	N	Mean (SD)
Age	72	74.96 (8.13)
MMSE score	72	28.39 (1.83)
IPL SUVr	59	1.52 (0.29)
MPF SUVr	59	1.46 (0.29)
MTL SUVr	40	1.3 (0.11)
PCC SUVr	67	1.55 (0.31)
Total intracranial volumes	72	1455.26 (132.46)
WMH volumes	69	4.43 (7.13)
Log WMH in SLF	55	1.12 (0.66)
Log WMH in IFOF	55	1.14 (0.65)
Log WMH in cingulum	25	0.92 (0.94)
Log WMH in cingulum hippocampus	25	0.95 (0.74)
APOE e4 allele N(%) copy1	71	7 (9.9%)
APOE e4 allele N(%) copy 2	71	26 (36.6%)
Sex male N (%)	72	37(49.3)

All the DMN SUVr values after excludes participants have SUVr less than 1.17
*Abbreviations: N: numbers; SD: standard deviation; SUVr: Standardized Uptake Value ratio; PCC: posterior cingulate; MPFC: medial prefrontal cortex ; IPL: inferior parietal lobules; MTL: medial temporal lobe; IFOF: inferior fronto-occipital fasciculus; SLF: superior longitudinal fasciculus; WMH: white matter hyperintensities ; MMSE: Mini-Mental State Examination

4.3.1 Association between WMH volume IN JHU-ICBM-tracts atlas and Aβ burden in DMN regions:

For each fiber tract, the linear regression analyses were computed, with Aβ within the tract's gray matter ROI as the dependent variable. The independent variable included WMH in each fiber tract, controlled for age, sex, ApoE and total intracranial volumes. The adjusted linear regression analyses demonstrated that increased WMH volumes in SLF was associated with

increased regional SUVr in IPL with p = 0.011 (Figure 4.2A). The analyses also detected marginally significant relation between MPF Aβ burdens with WMHs in IFOF (p value 0.074) (Figure 4.2B). In contrast, the regression models failed to detect significant relationships between the cingulum with PCC, or cingulum–hippocampus with MTL (p = 0.744 and 0.740 respectively) (Figures 4.2C and 4.2D) (Table 4.3).

Table 4.3 Independent effects of WMH IN JHU-ICBM-tracts atlas on DMN Aβ SUVr burden

DMN regions	WMH in JHU DTI-based white-matter atlases	Standardized Beta Coefficient	P-value	Adjusted R square
PCC SUVr	Cingulum	0.059	0.744	0.04
MTL SUVr	Cingulum hippocampus	0.054	0.740	0.10
IPL SUVr	SLF	0.365	0.011	0.19
MPF SUVr	IFOF	0.262	0.074	0.09

The adjusted R square is the proportion of variance in regional SUVr that was explained by the model discounted for age, sex, APOE and WMH volumes in JHU-DTI- based white matter atlastracts). (All coefficient β values are adjusted for the covariates age, sex, APOE and ICV)
*Abbreviations: Aβ: amyloid β; SUVr: Standardized Uptake Value ratio; PCC: posterior cingulate; MPFC: medial prefrontal cortex; IPL: inferior parietal lobules; MTL: medial temporal lobe; IFOF: inferior fronto-occipital fasciculus; SLF: superior longitudinal fasciculus; WMH: white matter hyperintensities; JHU-ICBM: Johns Hopkins University International Consortium for Brain Mapping probabilistic fiber tract atlas; DMN: default mode network.

Figure 4.2 Scatterplots show association between WMH volume IN JHU-ICBM-tracts atlas and Aβ burden in DMN regions
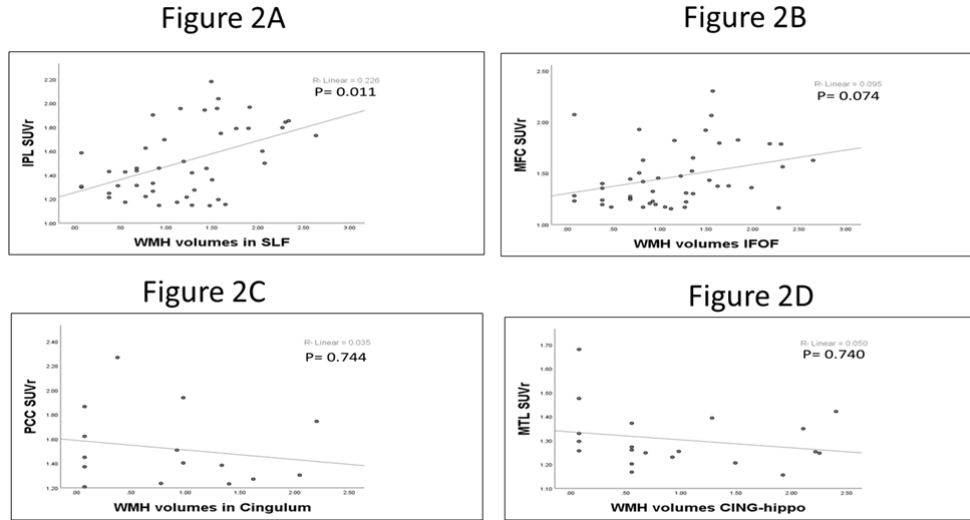
Figure 4.2 shows the scatterplot of the fitted regression line of the WMH volumes as independent variable and regional SUVr as the dependent variable. All p values are adjusted for the covariates age, sex, ApoE and total intracranial volumes. R square is the proportion of variance in the DMN regions SUVr that was explained by the WMH volumes in JHU-ICBM-tracts without any adjustment.
Abbreviations: Aβ: amyloid β; SUVr: Standardized Uptake Value ratio; PCC: posterior cingulate; MPFC: medial prefrontal cortex; IPL: inferior parietal lobules; MTL: medial temporal lobe; IFOF: inferior fronto-occipital fasciculus; SLF: superior longitudinal fasciculus; WMH: white matter hyperintensities; CING-hippo: cingulum–hippocampus tract.

4.4   Discussion:

The present data demonstrate that WMH volumes in major fiber tracts projecting from DMN regions are associated with upstream Aβ levels in connected DMN cortical regions. These data are consistent with recent studies demonstrating that WMH volumes in individual tracts explain more variance in the pathogenesis of AD than total or regional WMH burden, emphasizing the importance of lesion location when evaluating the clinical consequences of WMH [212]. These data suggest the possibility of a retrograde hypothesis wherein SVD in DMN pathways may lead to an upregulation of Aβ production in proximal neuronal cell bodies, initiating and or accelerating the pathogenesis of AD. Indeed, it is well established that ischemic injury proximal to neuronal cell bodies leads to an upregulation of Aβ production [213, 214], and so a retrograde hypothesis whereby more distal injury to connected axons, also leading to an

upregulation of Aβ production remains a plausible explanation for the association of AD and SVD seen across many studies [61, 132, 149] that is further supported by the present data.

In contrast to the present findings, a recent study that used ADNI (recruitment phases GO and II) found no association between the levels of global amyloid burden and WMH in any of the fiber tracts of the DMN [196]. The present study using regional amyloid burden rather than global measures of Aβ refines such analyses, establishing a direct relationship between WMH volumes in SLF and Aβ burden in IPL. A similar, albeit not statistically significant relationship was seen between WMH volumes in IFOF and Aβ burden in MPF. It is noteworthy that no such significant relationships were found between CING with PCC and CING-Hippo with MTL in the pAD cases studied. This discrepancy may be explained by understanding the neuroanatomic involvement of DMN regional involvement at distinct stages of AD, especially given that the present study sought to evaluate pAD specifically. Post-mortem pathologic studies have demonstrated that Aβ deposition follows a specific pattern of spread [215]. The topographical pattern of Aβ accumulation in pAD begins in the precuneus, medial orbitofrontal, and posterior cingulate cortices [5, 216-219], then the inferior parietal[102], and finally occipital and medial temporal lobes in the later stages of the disease. As such, in the pAD cohort studied, amyloid levels may have already reached a zenith in the PCC and may not have yet begun in the MTL narrowing the distributions of Aβ SUVr in these regions required to see associations with downstream tract WMH-mediated injury. Conversely, at the stage of pAD, accumulation of Aβ in the IPL and MPF cortices is an active process, broadening the distribution and allowing detection of the influences of WMH on Aβ accumulation in these DMN regions. Further work exploring the association of regional WMH and cortical Aβ deposition in connected DMN regions is needed to advance our understanding of the interplay between WMH and Aβ across the pathologic and clinical continuum of AD.

It is also possible that the involvement of only some DMN pathways could be due to the small sample size (only 25 participants) that had WMH involving the CING and CING-Hippo tracts. WMH affects WM tracts differently [212], some tracts, including IFOF and SLF, appear to be particularly vulnerable to WMH development compared to CING and CING-Hippo [196, 220]. It is also possible that these findings are related to the population studied, as ADNI excludes participants with significant vascular risk factors and or WMH burden that may limit analysis of the full impact of WMH within discrete WM tracts evident in a more generalizable population.

It is important to understand that the present study cannot determine causality as it investigated associations only. While our hypothesis is that WMH influences upstream Aβ deposition through increased Aβ production, it is also possible that Aβ -mediated neuronal injury leads to Wallerian degeneration, inflammation and or demyelination of axonal projection pathways that are supported by many prior studies [150, 221-225] that may eventually manifest as WMH in these DMN tracts. Indeed, WMH are not always caused by SVD, but are well recognized to be caused by Wallerian degeneration after any injury, inflammation in a variety of CNS diseases, and by the prototypic demyelination seen in multiple sclerosis and related disorders [226-228]. Unfortunately, definitive imaging characteristics distinguishing these causes of WMH are limited at present, further animal model work in the area of mixed AD-SVD is needed to explore the human associations demonstrated in the present study.

The main limitations of our study include the relatively small sample size available for this analysis from ADNI 3. Additional exploration after ADNI 3 and other cohorts with both Aβ- PET and 3D FLAIR is warranted. Another limitation of this study is applying an atlas-based fiber tract ROI approach to assessing DMN brain regions rather than using direct DTI measures. Due to natural variability in precise neuroanatomic localization of such pathways, it is possible that the true contributions of WMH within DMN tracts was over or underrepresented in specific individuals in the cohort. It should be noted, however, that an atlas-based approach has the advantage of avoiding problems of fiber tracking in degenerating pathways. Another major limitation of the present study is the selection bias as ADNI excludes participants with significant evidence for cerebrovascular disease, which may limit analysis of the full impact of WMH and other cerebrovascular injuries in relation to Aβ. Despite these limitations, it should be noted that focusing on the type, location, and connectivity of lesions rather than simply the presence or absence of lesions is the main strength of the present work.

In conclusion, the current results support the hypothesis of localized effects of WMH in axonal projections on cortical Aβ SUVr in DMN regions and tracts. Further studies testing our hypothesis at the level of microstructural damage are needed, especially given the findings from recent DTI studies demonstrating that WM microstructural alterations (even in the absence of overt WMH) are anatomically connected to the cortical brain regions with significant Aβ deposition at the earliest stages of disease within the DMN [100-102]. Further studies are also needed to define longitudinal patterns involved in the association of WMH on Aβ deposition in participants with mild cognitive impairment and dementia to allow a complete understanding of

the full disease course. Such work is critical for the optimal timing of disease modifying interventions that may target AD, SVD, and mixed pathologic processes that are most common in the general population.

CHAPTER 5.   THESIS SUMMARY, DISCUSSION AND FUTURE PERSPECTIVES

This thesis first tested the hypothesis that early focal regional amyloid deposition in the brain is associated with cognitive performance in specific cognitive domain scores in pAD (**chapter 2**). Since mixed dementia is widely recognized as the norm rather than the exception, the second study aimed to explore the potential causal relationships between regional and global Aβ and WMH with cognitive function (EF and memory) scores in CN older adults (**chapter 3**). Finally, the relationship between WMH and Aβ is strongly determined by the spatial distribution of the two pathologies, so the third study aimed to quantify Aβ in Default mode network (DMN) regions to examine whether cerebral small vessel disease (SVD) affects Aβ deposition in connected DMN regions (**chapter 4**).

5.1   The relation between Aβ and cognition in pAD

Previous studies evaluating the relationship between brain Aβ (measured on PET, or in CSF), and cognitive function have shown variation in the results in which cognitive domains are most affected by early Aβ deposition in pAD. Several such studies have demonstrated early memory decline in pAD [44-50], on contrary to deficits in EF or other domain involvement [51-55, 229]. These inconsistencies between studies could be due to the amyloid burden being often low or focal in pAD, and all of them used global rather than regional measures of Aβ deposition, which may limit detection of the earliest signs of Aβ pathology. Findings from clinical-pathological studies support the clinical meaningfulness of early regional Aβ deposition [124] and the predictive role of early precuneus pathology in the development of future global amyloid deposition in the brain and cognitive decline [123], steer the field toward studying the correlation between spatial distribution of Aβ and cognitive performance, especially in early pAD [5, 230].

Recent therapeutic attempts aiming at Aβ plaques have demonstrated limited success [231]. Potential reasons could include attempting anti-amyloid therapies too late in the disease course after downstream consequences on neurodegeneration and cognitive decline have taken hold [4]. Focusing on regional Aβ -PET SUVr levels in the precuneus and posterior cingulate demonstrates the benefit of using regional amyloid status rather than relying solely on global amyloid status to identify pAD for future amyloid targeted treatment studies and clinical trials.

A primary focus on memory domain impairment in relation to regional quantification of amyloid rather than examining a broader array of cognitive domain involvement [123-125] introduces bias that limits our complete understanding of the impact of early preclinical Aβ deposition. While the existing literature has shown that global Aβ burden has more robust associations with memory decline than any other cognitive domains in healthy older adults, the present data demonstrate that patients with early focal Aβ deposition have clinical features that differ from persons with more diffuse global Aβ [232]. The results from our first study clearly demonstrate that increased Aβ deposition in the precuneus and posterior cingulate (the earliest brain regions affected with Aβ pathology[3, 102]) are associated with changes in EF that may precede memory decline in pAD (Figure 5.1). Both posterior cingulate gyri and precuneus are highly anatomically connected [233], and are part of DMN that is involved in attention and executive function[234-236]. Moreover, Aβ accumulation in regions associated with DMN (i.e. the prefrontal cortex, inferior parietal lobule, posterior cingulate cortex, and precuneus) have been shown to be correlated with neuropsychological performance on multiple measures [230]. In summary, accumulating evidences from our study and two other independent samples [124, 237] indicate that assessing regional changes in amyloid, particularly in posterior cortical regions, enhances the early detection of subclinical amyloid-related cognitive decline.

Figure 5.1 Amyloid-PET levels in the Precuneus and Posterior Cingulate Cortices are Associated with Executive Function Scores in Preclinical Alzheimer`s Disease Prior to Overt Global Amyloid Positivity
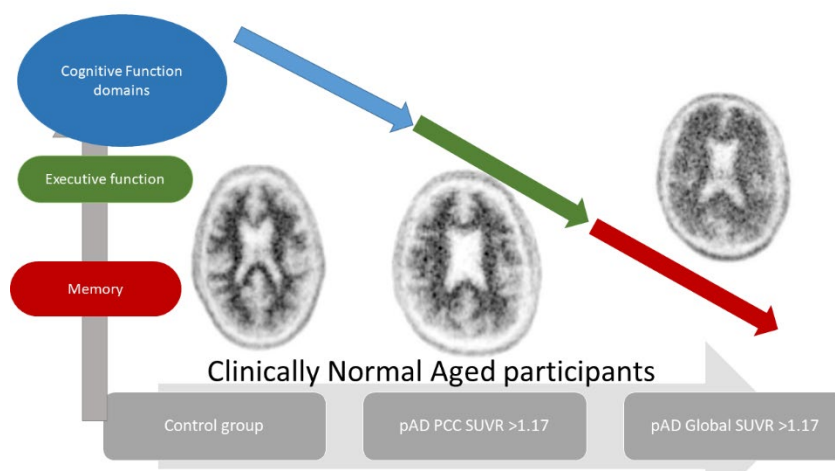
Regional amyloid deposition in the precuneus and posterior cingulate are associated with early preclinical decline in executive function in pAD, irrespective of global SUVr.
*Abbreviations Aβ: amyloid β, SUVr: Standardized Uptake Value ratio; pAD: preclinical Alzheimer's disease.

5.2 The relation between WMH burden, Aβ deposition, and cognition

EF refers to "higher-level" cognitive function [238]. Deficits in EF have been shown to predict the development of dementia [239-242] and are linked to both WMH burden and Aβ deposition in the brain [66, 71, 81, 243, 244]. EF performance is dependent on both intact white matter pathway connectivity, as well as pathologic integrity of the cortical regions themselves [167, 168]. The mechanisms contributing to EF decline in CN older adults are not fully understood and frequently overlap [66]. In fact, WMH burden and Aβ deposition are considered the two primary drivers of dementia and are associated with each other, suggesting a possible interaction of these two pathologies rather than a purely additive effect. (Figure 5.2)

Figure 5.2 Amyloid-PET and white matter hyperintensities have independent effects on baseline cognitive function and synergistic effects on longitudinal executive function
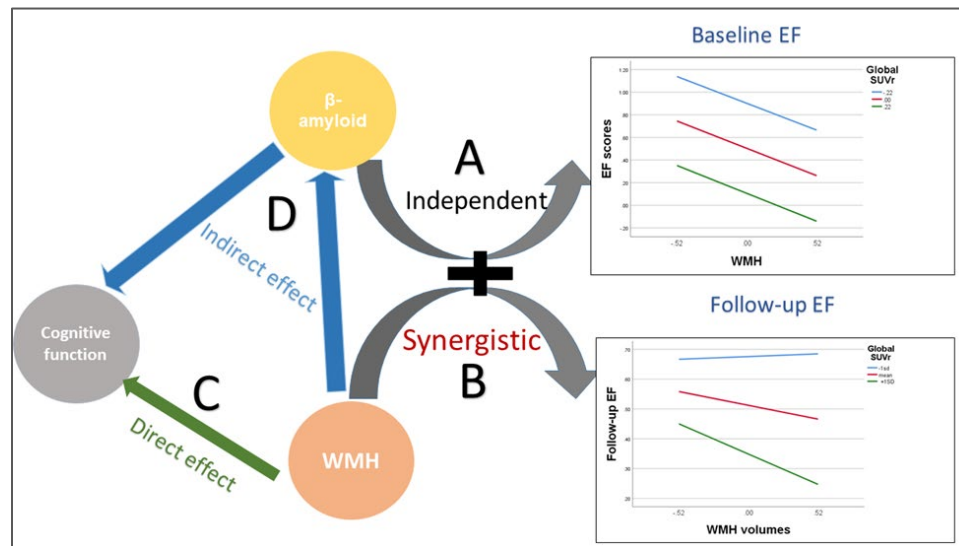
Aβ and WMHs contribute to baseline cognition independently (A), and there is a synergistic interaction between these baseline biomarkers of pathology on longitudinal EF performance (B). Furthermore, WMH dependent changes in cognitive performance are related to direct effect of WMH (C) and an indirect effect through both global and regional Aβ burden (D).

Data from our second study demonstrated that WMHs contribute to global pathology, exerting an effect on baseline cognitive performance through the direct effect of WMH and an indirect effect moderated through global and regional Aβ burden. The relationship between WMH and Aβ burden may be related to impaired general cerebral perfusion [74, 173] or to vascular pathology affecting amyloid clearance pathways [139], however the exact mechanisms remain unclear. Some preclinical studies suggest that WMHs may directly induce amyloid burden

[145, 146, 182, 183], and others have highlighted that baseline WMH predicted higher Aβ deposition over time [61, 147, 245]. It also remains possible that WMHs interact with the β-amyloid cascade at a mechanistic level[90]. The pathogenesis of both WMH and Aβ may involve a vicious circle, of which the initiating event remains unclear.

5.3   The spatial distribution and heterogeneity of WMH and Aβ

Evidence from recent studies has suggested that the relationship between WMH and Aβ is strongly determined by the spatial distribution of the two pathologies [150]. The majority of published studies have emphasized the spatial heterogeneity of WMH [98, 151]with posterior WMH predominance in relation to global Aβ measures [96-98, 145, 185]. Such prior studies have left the potential heterogeneous influences of regional Aβ deposition relatively unexplored. The topographic patterns of regional Aβ deposition in relation to WMH was investigated in chapter 3 of this thesis demonstrating that WMHs contribute to parietal and frontal Aβ burden. With these findings in mind and from a mechanistic point of view, there are many questions that remain unanswered. Why certain brain regions might be more vulnerable to WMH –related Aβ deposition, and are there biological mechanisms that can explain an interaction or are the observed associations simply due to confounding?

Recent studies on brain connectivity and functional neuroanatomy have resulted in a better understanding of the mechanism through which WMHs might lead to cognitive symptoms by disrupting the structurally connected cortical regions that represent the major networks of the brain [186, 187]. A possible mechanism explaining the contribution of WMH to the topographic pattern of Aβ may be due to the changes in structural connectivity in the frontal and frontal-parietal node [246, 247], which has been shown to lead to neuroinflammation that is hypothesized to spread trans-axonally to cortical regions [92, 190]. To explore the pathological interaction and biological link between WMH and Aβ within discrete WM tracts and cortical regions we conducted the third experiment.

The pathology underlying AD might be varied according to the Aβ regional distribution and is likely further influenced by WMH pathology [92]. WMH volumes in individual tracts explain more variance in the pathogenesis of AD than total or regional WMH [212]. With these data in mind, our third study demonstrates that increased WMH volumes in SLF was associated

with increased regional SUVr in IPL, supporting our contention that the WMH–Aβ relationship is region dependent. (Figure 5.3)

Figure 5.3 White Matter Hyperintensities Influence Distal Cortical β-Amyloid Accumulation in Defaults Mode Network Pathways
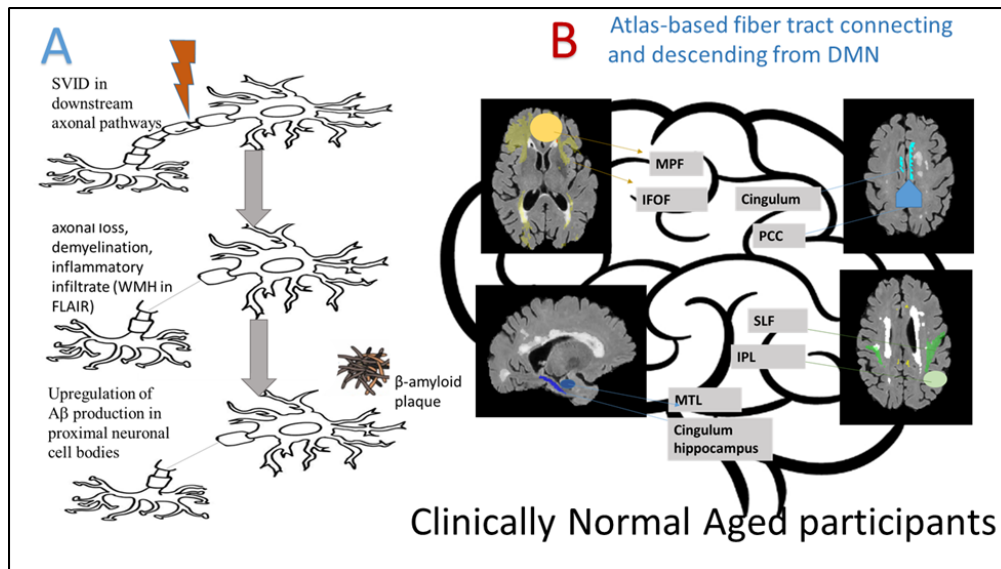
A: This study aimed to test the hypothesis that vascular injury (WMH) distal to the neuronal cell body, might upregulate amyloid production in connected cortical regions initiating and or accelerating the pathogenesis of AD in cognitively normal older adults with early Aβ deposition (pAD). B: After evaluation the association of WMH volumes in major fiber tracts projecting from cortical DMN regions and Aβ-PET SUVr in the connected cortical DMN regions, we found increased WMH volumes in the superior longitudinal fasciculus (SLF) was associated with increased regional SUVr in the inferior parietal lobule (IPL).

5.4   Conclusion

In conclusion, the results from the present set of experiments demonstrate that many factors may affect the interplay between Aβ and WMH during the preclinical phase of dementia. The first factor to consider is the temporal sequence and the spatial distribution of Aβ accumulation. Post-mortem pathologic studies showed that Aβ deposition follows a specific pattern of spread [215]. The topographical pattern of Aβ accumulation in pAD begins in the precuneus, medial orbitofrontal, and posterior cingulate cortices, spreading to core regions of the DMN [5, 216-219], then the inferior parietal[102], and finally occipital lobe, and temporal lobe in late stages of the disease. The data presented in this thesis demonstrate a significant association between WMH volumes in SLF and Aβ burden in IPL. In contrast, our studies failed to detect a

similar association in brain regions affected very early or late in the course of the disease. The second factor that needs to be understood involves the nature of the population studied. The majority of large-cohort studies in dementia that investigated the effects of WMH on neurodegeneration and cognition as ADNI excluded participants with severe vascular risk factors and considerable WMH burden (studies 2 and 3), which may limit analysis of the full impact of WMH and other cerebrovascular injuries in relation to Aβ. Finally, focusing on cognitively normal elderly participants affords an accurate and thorough understanding of the cognitive and brain changes accompanying pAD that is critical [248], however this approach limits the generalizability of the results, and it remains unclear how the relationships studied in this thesis might be altered at the later stages of mild cognitively impairment or in clinical AD patients. Molecular imaging studies of Aβ in pAD suggest that, on average, aged CN participants with pAD exhibit mean cortical levels of Aβ between those of healthy controls and AD patients.

5.5   Future direction and studies:

Neuroimaging data acquired at one point in time does not contain enough information to identify potential causal relationships between WMH and Aβ deposition. Further Longitudinal studies are needed to show that elevated WMH burden within discrete WM tracts at baseline worsened Aβ-PET SUVr in discrete cortical regions over time in AD cohorts. WM degeneration is a continuous process over time with microstructure alternation in WM integrity, which ultimately leads to macrostructure change, as reflected by WMH. Future investigations to evaluate Aβ SUVr in the cortical regions containing the neuron cell bodies that have preclinical WM alternation evidence (from DTI) to their downstream axon tracts are needed. Finally, further studies are needed to complete the dynamic understanding of WMH and Aβ pathology by exploring the interaction and spatial relation between the two pathologies in mild cognitively impaired or AD patients.

Initial Aβ deposition often falls below the global Aβ SUVr cut-off scores for the diagnosis of pAD and the majority of clinical trials. The field is at a crossroads about whether to continue to pursue anti-Aβ therapy or more actively pursue alternative targets for the pAD stage that may allow potentially more effective interventions with disease-modifying therapies that are on the horizon. The relation between Aβ and SVD in influencing executive function in pAD is partially driven directly by WMH and is additionally contributed to by WMH injury that accelerates Aβ deposition ultimately leading to the deficits in executive function seen in pAD. Efforts targeting

WMH may potentially augment and be needed in a staged approach in addition to anti-amyloid and other AD-focused disease modifying therapies.

REFERENCE

1. Rentz, D.M., et al., *Cognitive resilience in clinical and preclinical Alzheimer's disease: the Association of Amyloid and Tau Burden on cognitive performance.* Brain Imaging Behav, 2017. **11**(2): p. 383-390.
2. Ihara, R., et al., *Clinical and cognitive characteristics of preclinical Alzheimer's disease in the Japanese Alzheimer's Disease Neuroimaging Initiative cohort.* Alzheimers Dement (N Y), 2018. **4**: p. 645-651.
3. Villeneuve, S., et al., *Existing Pittsburgh Compound-B positron emission tomography thresholds are too high: statistical and pathological evaluation.* Brain, 2015. **138**(7): p. 2020-2033.
4. Teipel, S.J., et al., *In vivo staging of regional amyloid deposition predicts functional conversion in the preclinical and prodromal phases of Alzheimer's disease.* Neurobiology of aging, 2020. **93**: p. 98-108.
5. Grothe, M.J., et al., *In vivo staging of regional amyloid deposition.* Neurology, 2017. **89**(20): p. 2031-2038.
6. Markus, H.S. and R. Schmidt, *Genetics of vascular cognitive impairment.* Stroke, 2019. **50**(3): p. 765-772.
7. Cipollini, V., F. Troili, and F. Giubilei, *Emerging biomarkers in vascular cognitive impairment and dementia: from pathophysiological pathways to clinical application.* International journal of molecular sciences, 2019. **20**(11): p. 2812.
8. Dichgans, M. and D. Leys, *Vascular cognitive impairment.* Circulation research, 2017. **120**(3): p. 573-591.
9. Frantellizzi, V., et al., *Neuroimaging in vascular cognitive impairment and dementia: a systematic review.* Journal of Alzheimer's Disease, 2020. **73**(4): p. 1279-1294.
10. Gorelick, P.B., S.E. Counts, and D. Nyenhuis, *Vascular cognitive impairment and dementia.* Biochimica et Biophysica Acta (BBA)-Molecular Basis of Disease, 2016. **1862**(5): p. 860-868.
11. Rosenberg, G.A., M. Bjerke, and A. Wallin, *Multimodal markers of inflammation in the subcortical ischemic vascular disease type of vascular cognitive impairment.* Stroke, 2014. **45**(5): p. 1531-1538.
12. Vilar-Bergua, A., et al., *Blood and CSF biomarkers in brain subcortical ischemic vascular disease: involved pathways and clinical applicability.* Journal of Cerebral Blood Flow & Metabolism, 2016. **36**(1): p. 55-71.
13. Heiss, W.-D., et al., *Neuroimaging in vascular cognitive impairment: a state-of-the-art review.* BMC medicine, 2016. **14**(1): p. 1-8.
14. Staffaroni, A.M., et al. *Neuroimaging in dementia.* in *Seminars in neurology.* 2017. Thieme Medical Publishers.
15. Vitali, P., et al. *Neuroimaging in dementia.* in *Seminars in neurology.* 2008. © Thieme Medical Publishers.
16. Patel, K.P., et al., *Multimodality imaging of dementia: clinical importance and role of integrated anatomic and molecular imaging.* Radiographics, 2020. **40**(1): p. 200.
17. Ho, M.-L., *Arterial spin labeling: clinical applications.* Journal of Neuroradiology, 2018. **45**(5): p. 276-289.

18.   Ramin, S.L., W.A. Tognola, and A.R. Spotti, *Proton magnetic resonance spectroscopy: clinical applications in patients with brain lesions.* Sao Paulo Medical Journal, 2003. **121**: p. 254-259.

19.   Schaeffer, M.J., L. Chan, and P.A. Barber, *The neuroimaging of neurodegenerative and vascular disease in the secondary prevention of cognitive decline.* Neural Regeneration Research, 2021. **16**(8): p. 1490.

20.   Klunk, W.E., et al., *The Centiloid Project: standardizing quantitative amyloid plaque estimation by PET.* Alzheimer's & dementia, 2015. **11**(1): p. 1-15. e4.

21.   Yun, H.J., et al., *Centiloid method evaluation for amyloid PET of subcortical vascular dementia.* Scientific reports, 2017. **7**(1): p. 1-8.

22.   Wong, D.F., et al., *In vivo imaging of amyloid deposition in Alzheimer disease using the radioligand 18F-AV-45 (flobetapir F 18).* Journal of nuclear medicine, 2010. **51**(6): p. 913-920.

23.   Morris, E., et al., *Diagnostic accuracy of 18F amyloid PET tracers for the diagnosis of Alzheimer's disease: a systematic review and meta-analysis.* European journal of nuclear medicine and molecular imaging, 2016. **43**(2): p. 374-385.

24.   Su, Y., et al., *Quantitative analysis of PiB-PET with freesurfer ROIs.* PloS one, 2013. **8**(11): p. e73377.

25.   Mintun, M., et al., *[11C] PIB in a nondemented population: potential antecedent marker of Alzheimer disease.* Neurology, 2006. **67**(3): p. 446-452.

26.   Edison, P., et al., *Can target-to-pons ratio be used as a reliable method for the analysis of [11C] PIB brain scans?* Neuroimage, 2012. **60**(3): p. 1716-1723.

27.   Bullich, S., et al., *Optimal reference region to measure longitudinal amyloid-β change with 18F-Florbetaben PET.* Journal of Nuclear Medicine, 2017. **58**(8): p. 1300-1306.

28.   Barthel, H., et al. *PET/MR in dementia and other neurodegenerative diseases.* in *Seminars in nuclear medicine.* 2015. Elsevier.

29.   Cecchin, D., et al. *PET imaging in neurodegeneration and neuro-oncology: variants and pitfalls.* in *Seminars in nuclear medicine.* 2021. Elsevier.

30.   Schwarz, C.G., et al., *Contributions of imprecision in PET-MRI rigid registration to imprecision in amyloid PET SUVR measurements.* 2017, Wiley Online Library.

31.   Landau, S. and W. Jagust, *Florbetapir Processing Methods; 2015.* URL http://adni. bitbucket. org/docs/UCBERKELEYAV45/UCBERKELEY_AV45_Methods_12, 2015. **3**.

32.   Edison, P., et al., *Comparison of MRI based and PET template based approaches in the quantitative analysis of amyloid imaging with PIB-PET.* Neuroimage, 2013. **70**: p. 423-433.

33.   Schwarz, C.G., et al., *A large-scale comparison of cortical thickness and volume methods for measuring Alzheimer's disease severity.* NeuroImage: Clinical, 2016. **11**: p. 802-812.

34.   Schain, M., et al., *Evaluation of two automated methods for PET region of interest analysis.* Neuroinformatics, 2014. **12**(4): p. 551-562.

35.   Thurfjell, L., et al., *Automated quantification of 18F-flutemetamol PET activity for categorizing scans as negative or positive for brain amyloid: concordance with visual image reads.* Journal of Nuclear Medicine, 2014. **55**(10): p. 1623-1628.

36.   Zhou, L., et al., *MR-less surface-based amyloid assessment based on 11C PiB PET.* PLoS One, 2014. **9**(1): p. e84777.

37.   Alongi, P., et al., *18F-Florbetaben PET/CT to Assess Alzheimer's Disease: A new Analysis Method for Regional Amyloid Quantification.* Journal of Neuroimaging, 2019. **29**(3): p. 383-393.

38.   Bourgeat, P., et al., *Comparison of MR-less PiB SUVR quantification methods.* Neurobiology of aging, 2015. **36**: p. S159-S166.

39.   Schwarz, C.G., et al., *Optimizing PiB-PET SUVR change-over-time measurement by a large-scale analysis of longitudinal reliability, plausibility, separability, and correlation with MMSE.* Neuroimage, 2017. **144**: p. 113-127.

40.   Rullmann, M., et al., *Partial-volume effect correction improves quantitative analysis of 18F-florbetaben β-amyloid PET scans.* Journal of Nuclear Medicine, 2016. **57**(2): p. 198-203.

41.   Schwarz, C.G., et al., *A comparison of partial volume correction techniques for measuring change in serial amyloid PET SUVR.* Journal of Alzheimer's Disease, 2019. **67**(1): p. 181-195.

42.   Weintraub, S., et al., *Measuring cognition and function in the preclinical stage of Alzheimer's disease.* Alzheimers Dement (N Y), 2018. **4**: p. 64-75.

43.   Ko, H., et al., *Cognitive profiling related to cerebral amyloid beta burden using machine learning approaches.* Frontiers in aging neuroscience, 2019. **11**: p. 95.

44.   Rodrigue, K., et al., *β-Amyloid burden in healthy aging: regional distribution and cognitive consequences.* Neurology, 2012. **78**(6): p. 387-395.

45.   Riley, K.P., et al., *Prediction of preclinical Alzheimer's disease: longitudinal rates of change in cognition.* Journal of Alzheimer's Disease, 2011. **25**(4): p. 707-717.

46.   Lim, Y.Y., et al., *Rapid decline in episodic memory in healthy older adults with high amyloid-β.* Journal of Alzheimer's Disease, 2013. **33**(3): p. 675-679.

47.   Hedden, T., et al., *Meta-analysis of amyloid-cognition relations in cognitively normal older adults.* Neurology, 2013. **80**(14): p. 1341-1348.

48.   Ellis, K.A., et al., *Decline in cognitive function over 18 months in healthy older adults with high amyloid-β.* Journal of Alzheimer's Disease, 2013. **34**(4): p. 861-871.

49.   Monsell, S.E., et al., *Neuropsychological changes in asymptomatic persons with Alzheimer disease neuropathology.* Neurology, 2014. **83**(5): p. 434-440.

50.   Snitz, B.E., et al., *Cognitive trajectories associated with β-amyloid deposition in the oldest-old without dementia.* Neurology, 2013. **80**(15): p. 1378-1384.

51.   Pérez-Cordón, A., et al., *Subtle executive deficits are associated with higher brain amyloid burden and lower cortical volume in subjective cognitive decline: the FACEHBI cohort.* Scientific Reports, 2020. **10**(1): p. 1-8.

52.   Lim, Y.Y., et al., *Effect of amyloid on memory and non-memory decline from preclinical to clinical Alzheimer's disease.* Brain, 2014. **137**(1): p. 221-231.

53.   Harrington, M.G., et al., *Executive function changes before memory in preclinical Alzheimer's pathology: a prospective, cross-sectional, case control study.* PloS one, 2013. **8**(11): p. e79378.

54.   Mielke, M.M., et al., *Influence of amyloid and APOE on cognitive performance in a late middle-aged cohort.* Alzheimer's & Dementia, 2016. **12**(3): p. 281-291.

55.   Veitch, D.P., et al., *Understanding disease progression and improving Alzheimer's disease clinical trials: Recent highlights from the Alzheimer's Disease Neuroimaging Initiative.* Alzheimers Dement, 2019. **15**(1): p. 106-152.

56. Insel, P.S., et al., *The A4 study: β-amyloid and cognition in 4432 cognitively unimpaired adults.* Ann Clin Transl Neurol, 2020. **7**(5): p. 776-785.

57. Liu, W., et al., *Cerebrovascular disease, amyloid plaques, and dementia.* Stroke, 2015. **46**(5): p. 1402-7.

58. Kapasi, A., C. DeCarli, and J.A. Schneider, *Impact of multiple pathologies on the threshold for clinically overt dementia.* Acta Neuropathol, 2017. **134**(2): p. 171-186.

59. Park, J.-H., et al., *Effects of cerebrovascular disease and amyloid beta burden on cognition in subjects with subcortical vascular cognitive impairment.* Neurobiology of aging, 2014. **35**(1): p. 254-260.

60. Saridin, F.N., et al., *Brain amyloid β, cerebral small vessel disease, and cognition: a memory clinic study.* Neurology, 2020. **95**(21): p. e2845-e2853.

61. Kim, H.W., J. Hong, and J.C. Jeon, *Cerebral small vessel disease and Alzheimer's disease: a review.* Frontiers in Neurology, 2020. **11**: p. 927.

62. Wardlaw, J.M., C. Smith, and M. Dichgans, *Small vessel disease: mechanisms and clinical implications.* The Lancet Neurology, 2019. **18**(7): p. 684-696.

63. Caruso, P., R. Signori, and R. Moretti, *Small vessel disease to subcortical dementia: A dynamic model, which interfaces aging, cholinergic dysregulation and the neurovascular unit.* Vascular health and risk management, 2019. **15**: p. 259.

64. Maillard, P., et al., *FLAIR and diffusion MRI signals are independent predictors of white matter hyperintensities.* American Journal of Neuroradiology, 2013. **34**(1): p. 54-61.

65. Choi, H.-I., et al., *Changes in microvascular morphology in subcortical vascular dementia: a study of vessel size magnetic resonance imaging.* Frontiers in neurology, 2020. **11**: p. 545450.

66. Brown, C.A., et al., *Distinct patterns of default mode and executive control network circuitry contribute to present and future executive function in older adults.* Neuroimage, 2019. **195**: p. 320-332.

67. Gold, B.T., et al., *White matter integrity is associated with cerebrospinal fluid markers of Alzheimer's disease in normal adults.* Neurobiology of aging, 2014. **35**(10): p. 2263-2271.

68. DeCarli, C., P. Maillard, and E. Fletcher, *Four tissue segmentation in ADNI II.* Alzheimer's Disease Neuroimaging Initiative. Department of Neurology and Neurology and Center for Neuroscience, University of California at Davis. Available online: https://www. alz. washington. edu/WEB/adni_proto. pdf (accessed on 18 December 2013), 2013.

69. Bahrani, A.A., et al., *White matter hyperintensity associations with cerebral blood flow in elderly subjects stratified by cerebrovascular risk.* Journal of Stroke and Cerebrovascular Diseases, 2017. **26**(4): p. 779-786.

70. Bahrani, A.A., et al., *Post-acquisition processing confounds in brain volumetric quantification of white matter hyperintensities.* Journal of neuroscience methods, 2019. **327**: p. 108391.

71. Gold, B.T., et al., *Clinically silent Alzheimer's and vascular pathologies influence brain networks supporting executive function in healthy older adults.* Neurobiology of aging, 2017. **58**: p. 102-111.

72. Smith, C.D., et al., *Peripheral (deep) but not periventricular MRI white matter hyperintensities are increased in clinical vascular dementia compared to Alzheimer's disease.* Brain and behavior, 2016. **6**(3): p. e00438.

73. Attems, J. and K.A. Jellinger, *The overlap between vascular disease and Alzheimer's disease--lessons from pathology.* BMC Med, 2014. **12**: p. 206.

74. Iadecola, C., *The overlap between neurodegenerative and vascular factors in the pathogenesis of dementia.* Acta neuropathologica, 2010. **120**(3): p. 287-296.

75. Papma, J.M., et al., *Cerebral small vessel disease affects white matter microstructure in mild cognitive impairment.* Hum Brain Mapp, 2014. **35**(6): p. 2836-51.

76. Marchant, N.L., et al., *Cerebrovascular disease, beta-amyloid, and cognition in aging.* Neurobiology of aging, 2012. **33**(5): p. 1006. e25-1006. e36.

77. Vemuri, P., et al., *Vascular and amyloid pathologies are independent predictors of cognitive decline in normal elderly.* Brain, 2015. **138**(3): p. 761-771.

78. Marchant, N.L., et al., *The aging brain and cognition: contribution of vascular injury and aβ to mild cognitive dysfunction.* JAMA neurology, 2013. **70**(4): p. 488-495.

79. No, H.-J., et al., *Association between white matter lesions and cerebral glucose metabolism in patients with cognitive impairment.* Revista Española de Medicina Nuclear e Imagen Molecular (English Edition), 2019. **38**(3): p. 160-166.

80. Lee, M.J., et al., *Synergistic effects of ischemia and β-amyloid burden on cognitive decline in patients with subcortical vascular mild cognitive impairment.* JAMA psychiatry, 2014. **71**(4): p. 412-422.

81. Dupont, P.S., et al., *Amyloid burden and white matter hyperintensities mediate age-related cognitive differences.* Neurobiology of aging, 2020. **86**: p. 16-26.

82. Kuller, L., *Risk factors for dementia in the Cardiovascular Health Study cognition study.* Revista de neurologia, 2003. **37**(2): p. 122-126.

83. Hertze, J., et al., *Tau pathology and parietal white matter lesions have independent but synergistic effects on early development of Alzheimer's disease.* Dementia and geriatric cognitive disorders extra, 2013. **3**(1): p. 113-122.

84. Lindemer, E.R., et al., *White matter signal abnormality quality differentiates mild cognitive impairment that converts to Alzheimer's disease from nonconverters.* Neurobiology of aging, 2015. **36**(9): p. 2447-2457.

85. Ye, S., et al., *White-matter hyperintensities and lacunar infarcts are associated with an increased risk of Alzheimer's disease in the elderly in China.* Journal of Clinical Neurology, 2019. **15**(1): p. 46-53.

86. Kester, M.I., et al., *Associations between cerebral small-vessel disease and Alzheimer disease pathology as measured by cerebrospinal fluid biomarkers.* JAMA neurology, 2014. **71**(7): p. 855-862.

87. van Westen, D., et al., *Cerebral white matter lesions–associations with Aβ isoforms and amyloid PET.* Scientific reports, 2016. **6**(1): p. 1-9.

88. Moghekar, A., et al., *Cerebral white matter disease is associated with Alzheimer pathology in a prospective cohort.* Alzheimer's & Dementia, 2012. **8**: p. S71-S77.

89. Hardy, J. and D.J. Selkoe, *The amyloid hypothesis of Alzheimer's disease: progress and problems on the road to therapeutics.* science, 2002. **297**(5580): p. 353-356.

90. Garcia-Alloza, M., et al., *Cerebrovascular lesions induce transient β-amyloid deposition.* Brain, 2011. **134**(12): p. 3697-3707.

91. Kapasi, A. and J.A. Schneider, *Vascular contributions to cognitive impairment, clinical Alzheimer's disease, and dementia in older persons.* Biochim Biophys Acta, 2016. **1862**(5): p. 878-86.

92. Brickman, A.M., *Contemplating Alzheimer's disease and the contribution of white matter hyperintensities.* Current neurology and neuroscience reports, 2013. **13**(12): p. 1-9.

93.   Wolf, D., et al., *Non-linear association between cerebral amyloid deposition and white matter microstructure in cognitively healthy older adults.* Journal of Alzheimer's Disease, 2015. **47**(1): p. 117-127.

94.   Mito, R., et al., *Fibre-specific white matter reductions in Alzheimer's disease and mild cognitive impairment.* Brain, 2018. **141**(3): p. 888-902.

95.   Yoshita, M., et al., *Extent and distribution of white matter hyperintensities in normal aging, MCI, and AD.* Neurology, 2006. **67**(12): p. 2192-2198.

96.   Al-Janabi, O.M., et al., *Distinct White Matter Changes Associated with Cerebrospinal Fluid Amyloid-β 1-42 and Hypertension.* Journal of Alzheimer's Disease, 2018. **66**(3): p. 1095-1104.

97.   Garnier-Crussard, A., et al., *White matter hyperintensities across the adult lifespan: relation to age, Aβ load, and cognition.* Alzheimer's research & therapy, 2020. **12**(1): p. 1-11.

98.   Weaver, N.A., et al., *Cerebral amyloid burden is associated with white matter hyperintensity location in specific posterior white matter regions.* Neurobiology of aging, 2019. **84**: p. 225-234.

99.   Caballero, M.Á.A., et al., *Age-dependent amyloid deposition is associated with white matter alterations in cognitively normal adults during the adult life span.* Alzheimer's & Dementia, 2020. **16**(4): p. 651-661.

100.   Rieckmann, A., et al., *Accelerated decline in white matter integrity in clinically normal individuals at risk for Alzheimer's disease.* Neurobiology of aging, 2016. **42**: p. 177-188.

101.   Collij, L.E., et al., *White matter microstructure disruption in early stage amyloid pathology.* Alzheimer's & Dementia: Diagnosis, Assessment & Disease Monitoring, 2021. **13**(1): p. e12124.

102.   Palmqvist, S., et al., *Earliest accumulation of β-amyloid occurs within the default-mode network and concurrently affects brain connectivity.* Nature communications, 2017. **8**(1): p. 1-13.

103.   Weintraub, S., et al., *Version 3 of the Alzheimer Disease Centers' Neuropsychological Test Battery in the Uniform Data Set (UDS).* Alzheimer Dis Assoc Disord, 2018. **32**(1): p. 10-17.

104.   Nasreddine, Z.S., et al., *The Montreal Cognitive Assessment, MoCA: a brief screening tool for mild cognitive impairment.* J Am Geriatr Soc, 2005. **53**(4): p. 695-9.

105.   Delis, D.C., et al., *California verbal learning test.* Assessment, 2000.

106.   Luis, C.A., A.P. Keegan, and M. Mullan, *Cross validation of the Montreal Cognitive Assessment in community dwelling older adults residing in the Southeastern US.* International Journal of Geriatric Psychiatry: A journal of the psychiatry of late life and allied sciences, 2009. **24**(2): p. 197-201.

107.   Curry, S., et al., *Quantitative evaluation of beta-amyloid brain PET imaging in dementia: a comparison between two commercial software packages and the clinical report.* Br J Radiol, 2019. **92**(1101): p. 20181025.

108.   Fleisher, A.S., et al., *Using positron emission tomography and florbetapir F 18 to image cortical amyloid in patients with mild cognitive impairment or dementia due to Alzheimer disease.* Archives of neurology, 2011. **68**(11): p. 1404-1411.

109.   Clark, C.M., et al., *Use of florbetapir-PET for imaging β-amyloid pathology.* Jama, 2011. **305**(3): p. 275-283.

110. Charidimou, A., et al., *Amyloid-PET burden and regional distribution in cerebral amyloid angiopathy: a systematic review and meta-analysis of biomarker performance.* Journal of Neurology, Neurosurgery & Psychiatry, 2018. **89**(4): p. 410-417.

111. Attems, J., et al., *Topographical distribution of cerebral amyloid angiopathy and its effect on cognitive decline are influenced by Alzheimer disease pathology.* Journal of the neurological sciences, 2007. **257**(1-2): p. 49-55.

112. Adams, M.C., et al., *A systematic review of the factors affecting accuracy of SUV measurements.* American Journal of Roentgenology, 2010. **195**(2): p. 310-320.

113. Catafau, A.M., et al., *Cerebellar amyloid-β plaques: How frequent are they, and do they influence 18F-florbetaben SUV ratios?* Journal of Nuclear Medicine, 2016. **57**(11): p. 1740-1745.

114. Insel, P.S., O. Hansson, and N. Mattsson-Carlgren, *Association between apolipoprotein E ε2 vs ε4, age, and β-amyloid in adults without cognitive impairment.* JAMA neurology, 2021. **78**(2): p. 229-235.

115. Promteangtrong, C., et al., *Multimodality imaging approaches in Alzheimer's disease. Part II: 1H MR spectroscopy, FDG PET and Amyloid PET.* Dementia & neuropsychologia, 2015. **9**: p. 330-342.

116. Fan, L.-Y., et al., *The relation between brain amyloid deposition, cortical atrophy, and plasma biomarkers in amnesic mild cognitive impairment and Alzheimer's disease.* Frontiers in aging neuroscience, 2018. **10**: p. 175.

117. Gili, T., et al., *Regional brain atrophy and functional disconnection across Alzheimer's disease evolution.* Journal of Neurology, Neurosurgery & Psychiatry, 2011. **82**(1): p. 58-66.

118. Teipel, S., M.J. Grothe, and A.s.D.N. Initiative, *Does posterior cingulate hypometabolism result from disconnection or local pathology across preclinical and clinical stages of Alzheimer's disease?* European journal of nuclear medicine and molecular imaging, 2016. **43**(3): p. 526-536.

119. Bowie, C.R. and P.D. Harvey, *Administration and interpretation of the Trail Making Test.* Nature protocols, 2006. **1**(5): p. 2277.

120. Ritter, A., et al., *The Association between Montreal Cognitive Assessment Memory Scores and Hippocampal Volume in a Neurodegenerative Disease Sample.* J Alzheimers Dis, 2017. **58**(3): p. 695-699.

121. Bickford, D., et al., *Screening for Executive Dysfunction in Late-Life Depression: Utility of Trail Making Test and Self-Report Measures.* Am J Geriatr Psychiatry, 2018. **26**(10): p. 1091-1094.

122. Levin, F., et al., *In vivo staging of regional amyloid progression in healthy middle-aged to older people at risk of Alzheimer's disease.* Alzheimers Res Ther, 2021. **13**(1): p. 178.

123. Collij, L.E., et al., *Regional amyloid accumulation predicts memory decline in initially cognitively unimpaired individuals.* Alzheimers Dement (Amst), 2021. **13**(1): p. e12216.

124. Farrell, M.E., et al., *Regional amyloid accumulation and cognitive decline in initially amyloid-negative adults.* Neurology, 2018. **91**(19): p. e1809-e1821.

125. Perrotin, A., et al., *Subjective cognition and amyloid deposition imaging: a Pittsburgh Compound B positron emission tomography study in normal elderly individuals.* Arch Neurol, 2012. **69**(2): p. 223-9.

126. Gottesman, R.F., et al., *The ARIC-PET amyloid imaging study: brain amyloid differences by age, race, sex, and APOE.* Neurology, 2016. **87**(5): p. 473-480.

127. Kawas, C.H., et al., *Amyloid imaging and cognitive decline in nondemented oldest-old: the 90+ Study.* Alzheimer's & Dementia, 2013. **9**(2): p. 199-203.

128. Vemuri, P., et al., *Tau-PET uptake: regional variation in average SUVR and impact of amyloid deposition.* Alzheimer's & Dementia: Diagnosis, Assessment & Disease Monitoring, 2017. **6**: p. 21-30.

129. Hammond, T.C., et al., *β-amyloid and tau drive early Alzheimer's disease decline while glucose hypometabolism drives late decline.* Communications biology, 2020. **3**(1): p. 1-13.

130. Qin, Q., et al., *Default mode network integrity changes contribute to cognitive deficits in subcortical vascular cognitive impairment, no dementia.* Brain Imaging Behav, 2021. **15**(1): p. 255-265.

131. Chen, X.-Q. and W.C. Mobley, *Alzheimer disease pathogenesis: insights from molecular and cellular biology studies of oligomeric Aβ and tau species.* Frontiers in Neuroscience, 2019. **13**: p. 659.

132. Kanaan, N.M., et al., *Axonal degeneration in Alzheimer's disease: when signaling abnormalities meet the axonal transport system.* Experimental neurology, 2013. **246**: p. 44-53.

133. Zukotynski, K., et al., *The use of random forests to identify brain regions on amyloid and FDG PET associated with MoCA score.* Clinical nuclear medicine, 2020. **45**(6): p. 427-433.

134. Rosenberg, P.B., et al., *Cognition and amyloid load in Alzheimer disease imaged with florbetapir F 18(AV-45) positron emission tomography.* Am J Geriatr Psychiatry, 2013. **21**(3): p. 272-8.

135. Chui, H.C. and L. Ramirez-Gomez, *Clinical and imaging features of mixed Alzheimer and vascular pathologies.* Alzheimer's research & therapy, 2015. **7**(1): p. 21.

136. Sato, N. and R. Morishita, *The roles of lipid and glucose metabolism in modulation of β-amyloid, tau, and neurodegeneration in the pathogenesis of Alzheimer disease.* Front Aging Neurosci, 2015. **7**: p. 199.

137. Schneider, J.A., et al., *Mixed brain pathologies account for most dementia cases in community-dwelling older persons.* Neurology, 2007. **69**(24): p. 2197-204.

138. Hedden, T., et al., *Cognitive profile of amyloid burden and white matter hyperintensities in cognitively normal older adults.* Journal of Neuroscience, 2012. **32**(46): p. 16233-16242.

139. Roseborough, A., et al., *Associations between amyloid β and white matter hyperintensities: a systematic review.* Alzheimer's & Dementia, 2017. **13**(10): p. 1154-1167.

140. Han, J.W., et al., *Association of vascular brain injury, neurodegeneration, amyloid, and cognitive trajectory.* Neurology, 2020. **95**(19): p. e2622-e2634.

141. Kim, H.J., et al., *Clinical effect of white matter network disruption related to amyloid and small vessel disease.* Neurology, 2015. **85**(1): p. 63-70.

142. Brugulat-Serrat, A., et al., *Patterns of white matter hyperintensities associated with cognition in middle-aged cognitively healthy individuals.* Brain imaging and behavior, 2020. **14**(5): p. 2012-2023.

143. Tullberg, M., et al., *White matter lesions impair frontal lobe function regardless of their location.* Neurology, 2004. **63**(2): p. 246-53.

144. Jack, C.R., Jr., et al., *Tracking pathophysiological processes in Alzheimer's disease: an updated hypothetical model of dynamic biomarkers.* Lancet Neurol, 2013. **12**(2): p. 207-16.

145.   Lee, S., et al., *White matter hyperintensities are a core feature of Alzheimer's disease: evidence from the dominantly inherited Alzheimer network.* Annals of neurology, 2016. **79**(6): p. 929-939.

146.   Iturria-Medina, Y., et al., *Early role of vascular dysregulation on late-onset Alzheimer's disease based on multifactorial data-driven analysis.* Nat Commun, 2016. **7**: p. 11934.

147.   Moscoso, A., et al., *White matter hyperintensities are associated with subthreshold amyloid accumulation.* Neuroimage, 2020. **218**: p. 116944.

148.   Kanaan, N.M., et al., *Axonal degeneration in Alzheimer's disease: when signaling abnormalities meet the axonal transport system.* Exp Neurol, 2013. **246**: p. 44-53.

149.   Salvadores, N., C. Gerónimo-Olvera, and F.A. Court, *Axonal degeneration in AD: the contribution of Aβ and Tau.* Frontiers in Aging Neuroscience, 2020. **12**: p. 581767.

150.   Lorenzini, L., et al., *Regional associations of white matter hyperintensities and early cortical amyloid pathology.* Brain communications, 2022. **4**(3): p. fcac150.

151.   Pålhaugen, L., et al., *Brain amyloid and vascular risk are related to distinct white matter hyperintensity patterns.* Journal of Cerebral Blood Flow & Metabolism, 2021. **41**(5): p. 1162-1174.

152.   Mueller, S.G., et al., *Ways toward an early diagnosis in Alzheimer's disease: the Alzheimer's Disease Neuroimaging Initiative (ADNI).* Alzheimer's & Dementia, 2005. **1**(1): p. 55-66.

153.   Jack Jr, C.R., et al., *The Alzheimer's disease neuroimaging initiative (ADNI): MRI methods.* Journal of Magnetic Resonance Imaging: An Official Journal of the International Society for Magnetic Resonance in Medicine, 2008. **27**(4): p. 685-691.

154.   Petersen, R.C., et al., *Alzheimer's disease neuroimaging initiative (ADNI): clinical characterization.* Neurology, 2010. **74**(3): p. 201-209.

155.   Jenkinson, M., et al., *Fsl.* Neuroimage, 2012. **62**(2): p. 782-790.

156.   Smith, S.M., et al., *Advances in functional and structural MR image analysis and implementation as FSL.* Neuroimage, 2004. **23**: p. S208-S219.

157.   Jagust, W.J., et al., *The Alzheimer's disease neuroimaging initiative 2 PET core: 2015.* Alzheimer's & Dementia, 2015. **11**(7): p. 757-771.

158.   Fischl, B., M.I. Sereno, and A.M. Dale, *Cortical surface-based analysis: II: inflation, flattening, and a surface-based coordinate system.* Neuroimage, 1999. **9**(2): p. 195-207.

159.   Fischl, B., et al., *Whole brain segmentation: automated labeling of neuroanatomical structures in the human brain.* Neuron, 2002. **33**(3): p. 341-355.

160.   Nowrangi, M.A., et al., *Systematic review of neuroimaging correlates of executive functioning: converging evidence from different clinical populations.* J Neuropsychiatry Clin Neurosci, 2014. **26**(2): p. 114-25.

161.   Ranasinghe, K.G., et al., *Regional functional connectivity predicts distinct cognitive impairments in Alzheimer's disease spectrum.* Neuroimage Clin, 2014. **5**: p. 385-95.

162.   Ali, D.G., et al., *Amyloid-PET Levels in the Precuneus and Posterior Cingulate Cortices Are Associated with Executive Function Scores in Preclinical Alzheimer's Disease Prior to Overt Global Amyloid Positivity.* Journal of Alzheimer's Disease, 2022(Preprint): p. 1-9.

163.   Gibbons, L.E., et al., *Composite measures of executive function and memory: ADNI_EF and ADNI_Mem.* Alzheimer's Dis Neuroimaging Initiat, 2012.

164.   Hayes, A.F., *Introduction to mediation, moderation, and conditional process analysis: A regression-based approach.* 2017: Guilford publications.

165. Carmichael, O., et al., *MRI predictors of cognitive change in a diverse and carefully characterized elderly population.* Neurobiology of aging, 2012. **33**(1): p. 83-95. e2.

166. Lin, C., et al., *The effect of amyloid deposition on longitudinal resting-state functional connectivity in cognitively normal older adults.* Alzheimers Res Ther, 2020. **12**(1): p. 7.

167. Wang, Z., et al., *The effect of white matter signal abnormalities on default mode network connectivity in mild cognitive impairment.* Human brain mapping, 2020. **41**(5): p. 1237-1248.

168. Kumar, D., et al., *Differential Effects of Confluent and Nonconfluent White Matter Hyperintensities on Functional Connectivity in Mild Cognitive Impairment.* Brain Connectivity, 2020. **10**(10): p. 547-554.

169. Maillard, P., et al., *Coevolution of white matter hyperintensities and cognition in the elderly.* Neurology, 2012. **79**(5): p. 442-448.

170. Carey, C.L., et al., *Subcortical lacunes are associated with executive dysfunction in cognitively normal elderly.* Stroke, 2008. **39**(2): p. 397-402.

171. Kumar, D., et al., *APOE4 and Confluent White Matter Hyperintensities Have a Synergistic Effect on Episodic Memory Impairment in Prodromal Dementia.* Journal of Alzheimer's Disease, 2022(Preprint): p. 1-12.

172. Ottoy, J., et al., *Vascular burden and cognition: Mediating roles of neurodegeneration and amyloid PET.* Alzheimers Dement, 2022.

173. Zlokovic, B.V., *Neurovascular pathways to neurodegeneration in Alzheimer's disease and other disorders.* Nature Reviews Neuroscience, 2011. **12**(12): p. 723-738.

174. Park, M., et al., *Myelin loss in white matter hyperintensities and normal-appearing white matter of cognitively impaired patients: a quantitative synthetic magnetic resonance imaging study.* Eur Radiol, 2019. **29**(9): p. 4914-4921.

175. Bartzokis, G., *Alzheimer's disease as homeostatic responses to age-related myelin breakdown.* Neurobiol Aging, 2011. **32**(8): p. 1341-71.

176. CENTER, P.C.C. and N.B. CORE, *Alzheimer's Disease Neuroimaging Initiative 2 (ADNI2) Protocol (ADC-039).* 2014, Citeseer.

177. Honjo, K., S.E. Black, and N.P. Verhoeff, *Alzheimer's disease, cerebrovascular disease, and the β-amyloid cascade.* Canadian Journal of Neurological Sciences, 2012. **39**(6): p. 712-728.

178. Ortner, M., et al., *Small vessel disease, but neither amyloid load nor metabolic deficit, is dependent on age at onset in Alzheimer's disease.* Biological psychiatry, 2015. **77**(8): p. 704-710.

179. Noh, Y., et al., *White matter hyperintensities are associated with amyloid burden in APOE4 non-carriers.* Journal of Alzheimer's Disease, 2014. **40**(4): p. 877-886.

180. Kim, H.J., et al., *Relative impact of amyloid-β, lacunes, and downstream imaging markers on cognitive trajectories.* Brain, 2016. **139**(9): p. 2516-2527.

181. Yi, H.-A., et al., *Association between white matter lesions and cerebral Aβ burden.* PloS one, 2018. **13**(9): p. e0204313.

182. Sachdev, P.S., et al., *Is Alzheimer's a disease of the white matter?* Current opinion in psychiatry, 2013. **26**(3): p. 244-251.

183. Yew, B. and D.A. Nation, *Cerebrovascular resistance: effects on cognitive decline, cortical atrophy, and progression to dementia.* Brain, 2017. **140**(7): p. 1987-2001.

184. Zhou, Y., F. Yu, and T.Q. Duong, *White matter lesion load is associated with resting state functional MRI activity and amyloid PET but not FDG in mild cognitive impairment and early Alzheimer's disease patients.* J Magn Reson Imaging, 2015. **41**(1): p. 102-9.

185. Graff-Radford, J., et al., *White matter hyperintensities: relationship to amyloid and tau burden.* Brain, 2019. **142**(8): p. 2483-2491.

186. Ter Telgte, A., et al., *Cerebral small vessel disease: from a focal to a global perspective.* Nature Reviews Neurology, 2018. **14**(7): p. 387-398.

187. Tuladhar, A.M., et al., *Structural network connectivity and cognition in cerebral small vessel disease.* Human brain mapping, 2016. **37**(1): p. 300-310.

188. Radlinska, B.A., et al., *Changes in callosal motor fiber integrity after subcortical stroke of the pyramidal tract.* Journal of Cerebral Blood Flow & Metabolism, 2012. **32**(8): p. 1515-1524.

189. Ly, J.V., et al., *Subacute ischemic stroke is associated with focal 11C PiB positron emission tomography retention but not with global neocortical Aβ deposition.* Stroke, 2012. **43**(5): p. 1341-1346.

190. Thiel, A., et al., *Amyloid burden, neuroinflammation, and links to cognitive decline after ischemic stroke.* Stroke, 2014. **45**(9): p. 2825-2829.

191. Simic, G., et al., *Early failure of the default-mode network and the pathogenesis of Alzheimer's disease.* CNS neuroscience & therapeutics, 2014. **20**(7): p. 692.

192. Brown, C.A., et al., *Age and Alzheimer's pathology disrupt default mode network functioning via alterations in white matter microstructure but not hyperintensities.* Cortex, 2018. **104**: p. 58-74.

193. Mito, R., et al., *Fibre-specific white matter reductions in Alzheimer's disease and mild cognitive impairment.* Brain, 2018. **141**(3): p. 888-902.

194. Habes, M., et al., *White matter hyperintensities and imaging patterns of brain ageing in the general population.* Brain, 2016. **139**(4): p. 1164-1179.

195. Jacobs, H.I., et al., *The association between white matter hyperintensities and executive decline in mild cognitive impairment is network dependent.* Neurobiology of aging, 2012. **33**(1): p. 201. e1-201. e8.

196. Taylor, A.N., et al., *Tract-specific white matter hyperintensities disrupt neural network function in Alzheimer's disease.* Alzheimer's & Dementia, 2017. **13**(3): p. 225-235.

197. Weiler, M., et al., *Structural connectivity of the default mode network and cognition in Alzheimer's disease.* Psychiatry Res, 2014. **223**(1): p. 15-22.

198. Jenkinson, M., et al., *Improved optimization for the robust and accurate linear registration and motion correction of brain images.* Neuroimage, 2002. **17**(2): p. 825-841.

199. Greve, D.N., et al., *Different partial volume correction methods lead to different conclusions: an 18F-FDG-PET study of aging.* Neuroimage, 2016. **132**: p. 334-343.

200. Greve, D.N., et al., *Cortical surface-based analysis reduces bias and variance in kinetic modeling of brain PET data.* Neuroimage, 2014. **92**: p. 225-236.

201. Hua, K., et al., *Tract probability maps in stereotaxic spaces: analyses of white matter anatomy and tract-specific quantification.* Neuroimage, 2008. **39**(1): p. 336-347.

202. Whitfield-Gabrieli, S. and J.M. Ford, *Default mode network activity and connectivity in psychopathology.* Annual review of clinical psychology, 2012. **8**: p. 49-76.

203. Wu, Y., et al., *Segmentation of the cingulum bundle in the human brain: a new perspective based on DSI tractography and fiber dissection study.* Frontiers in neuroanatomy, 2016. **10**: p. 84.

204. Chen, X., et al., *Disrupted functional and structural connectivity within default mode network contribute to WMH-related cognitive impairment.* Neuroimage Clin, 2019. **24**: p. 102088.

205. Hodgetts, C.J., et al., *Increased posterior default mode network activity and structural connectivity in young adult APOE-ε4 carriers: a multimodal imaging investigation.* Neurobiol Aging, 2019. **73**: p. 82-91.

206. Barbeau, E.B., M. Descoteaux, and M. Petrides, *Dissociating the white matter tracts connecting the temporo-parietal cortical region with frontal cortex using diffusion tractography.* Scientific reports, 2020. **10**(1): p. 1-13.

207. Araque Caballero, M.Á., et al., *White matter diffusion alterations precede symptom onset in autosomal dominant Alzheimer's disease.* Brain, 2018. **141**(10): p. 3065-3080.

208. Burks, J.D., et al., *Anatomy and white matter connections of the orbitofrontal gyrus.* Journal of neurosurgery, 2017. **128**(6): p. 1865-1872.

209. Van Den Heuvel, M.P., et al., *Functionally linked resting-state networks reflect the underlying structural connectivity architecture of the human brain.* Human brain mapping, 2009. **30**(10): p. 3127-3141.

210. Damoiseaux, J.S. and M.D. Greicius, *Greater than the sum of its parts: a review of studies combining structural connectivity and resting-state functional connectivity.* Brain structure and function, 2009. **213**(6): p. 525-533.

211. Greicius, M.D., et al., *Resting-state functional connectivity reflects structural connectivity in the default mode network.* Cerebral cortex, 2009. **19**(1): p. 72-78.

212. Seiler, S., et al., *Cerebral tract integrity relates to white matter hyperintensities, cortex volume, and cognition.* Neurobiology of aging, 2018. **72**: p. 14-22.

213. Pluta, R., et al., *Sporadic Alzheimer's disease begins as episodes of brain ischemia and ischemically dysregulated Alzheimer's disease genes.* Molecular neurobiology, 2013. **48**(3): p. 500-515.

214. Pluta, R., et al., *Participation of amyloid and tau protein in neuronal death and neurodegeneration after brain ischemia.* International Journal of Molecular Sciences, 2020. **21**(13): p. 4599.

215. Thal, D.R., et al., *Phases of Aβ-deposition in the human brain and its relevance for the development of AD.* Neurology, 2002. **58**(12): p. 1791-1800.

216. Cho, H., et al., *In vivo cortical spreading pattern of tau and amyloid in the Alzheimer disease spectrum.* Annals of neurology, 2016. **80**(2): p. 247-258.

217. Mattsson, N., et al., *Staging β-amyloid pathology with amyloid positron emission tomography.* JAMA neurology, 2019. **76**(11): p. 1319-1329.

218. Pfeil, J., et al., *Unique regional patterns of amyloid burden predict progression to prodromal and clinical stages of Alzheimer's disease.* Neurobiology of aging, 2021. **106**: p. 119-129.

219. Sakr, F.A., et al., *Applicability of in vivo staging of regional amyloid burden in a cognitively normal cohort with subjective memory complaints: the INSIGHT-preAD study.* Alzheimer's research & therapy, 2019. **11**(1): p. 1-11.

220. Petersen, M., et al., *Fixel based analysis of white matter alterations in early stage cerebral small vessel disease.* Scientific reports, 2022. **12**(1): p. 1-12.

221. McAleese, K.E., et al., *Parietal white matter lesions in Alzheimer's disease are associated with cortical neurodegenerative pathology, but not with small vessel disease.* Acta neuropathologica, 2017. **134**(3): p. 459-473.

222. Alber, J., et al., *White matter hyperintensities in vascular contributions to cognitive impairment and dementia (VCID): Knowledge gaps and opportunities.* Alzheimer's & Dementia: Translational Research & Clinical Interventions, 2019. **5**: p. 107-117.

223. Dadar, M., et al., *The temporal relationships between white matter hyperintensities, neurodegeneration, amyloid beta, and cognition.* Alzheimer's & Dementia: Diagnosis, Assessment & Disease Monitoring, 2020. **12**(1): p. e12091.

224. Schoemaker, D., et al., *White matter hyperintensities are a prominent feature of autosomal dominant Alzheimer's disease that emerge prior to dementia.* Alzheimer's Research & Therapy, 2022. **14**(1): p. 1-11.

225. Phuah, C.-L., et al., *Association of Data-Driven White Matter Hyperintensity Spatial Signatures With Distinct Cerebral Small Vessel Disease Etiologies.* Neurology, 2022.

226. Medana, I. and M. Esiri, *Axonal damage: a key predictor of outcome in human CNS diseases.* Brain, 2003. **126**(3): p. 515-530.

227. Leys, D., et al., *Could Wallerian degeneration contribute to" leuko-araiosis" in subjects free of any vascular disorder?* Journal of Neurology, Neurosurgery & Psychiatry, 1991. **54**(1): p. 46-50.

228. Rotshenker, S., *Wallerian degeneration: the innate-immune response to traumatic nerve injury.* Journal of neuroinflammation, 2011. **8**(1): p. 1-14.

229. Wilson, R.S., et al., *Cognitive decline in prodromal Alzheimer disease and mild cognitive impairment.* Archives of neurology, 2011. **68**(3): p. 351-356.

230. Stevens, D.A., et al., *Regional amyloid correlates of cognitive performance in ageing and mild cognitive impairment.* Brain communications, 2022. **4**(1): p. fcac016.

231. Avgerinos, K.I., L. Ferrucci, and D. Kapogiannis, *Effects of monoclonal antibodies against amyloid-β on clinical and biomarker outcomes and adverse event risks: A systematic review and meta-analysis of phase III RCTs in Alzheimer's disease.* Ageing Research Reviews, 2021. **68**: p. 101339.

232. Kim, S.E., et al., *Clinical significance of focal ß-amyloid deposition measured by (18)F-flutemetamol PET.* Alzheimers Res Ther, 2020. **12**(1): p. 6.

233. Leech, R. and D.J. Sharp, *The role of the posterior cingulate cortex in cognition and disease.* Brain, 2014. **137**(1): p. 12-32.

234. Beaty, R.E., et al., *Default and executive network coupling supports creative idea production.* Scientific reports, 2015. **5**(1): p. 1-14.

235. Connolly, J., et al., *Identification of resting state networks involved in executive function.* Brain connectivity, 2016. **6**(5): p. 365-374.

236. Qin, Q., et al., *Default mode network integrity changes contribute to cognitive deficits in subcortical vascular cognitive impairment, no dementia.* Brain Imaging and Behavior, 2021. **15**(1): p. 255-265.

237. Landau, S.M., et al., *Memory decline accompanies subthreshold amyloid accumulation.* Neurology, 2018. **90**(17): p. e1452-e1460.

238. Kim, S., et al., *Disproportionate Decline of Executive Functions in Early Mild Cognitive Impairment, Late Mild Cognitive Impairment, and Mild Alzheimer's Disease.* Dement Neurocogn Disord, 2016. **15**(4): p. 159-164.

239. Clark, L.R., et al., *Specific measures of executive function predict cognitive decline in older adults.* Journal of the International Neuropsychological Society, 2012. **18**(1): p. 118.

240. Seo, E.H., et al., *Altered Executive Function in Pre-Mild Cognitive Impairment.* J Alzheimers Dis, 2016. **54**(3): p. 933-940.

241. Ewers, M., et al., *Reduced FDG-PET brain metabolism and executive function predict clinical progression in elderly healthy subjects.* Neuroimage Clin, 2014. **4**: p. 45-52.
242. Rajan, K.B., et al., *Cognitive impairment 18 years before clinical diagnosis of Alzheimer disease dementia.* Neurology, 2015. **85**(10): p. 898-904.
243. Onami, S., *The Aging Brain: Are two pathologies worse than one? White matter hyperintensities, beta-amyloid, and cognition in normal elderly.* Berkeley Scientific Journal, 2010. **13**(2).
244. Camerino, I., et al., *White matter hyperintensities at critical crossroads for executive function and verbal abilities in small vessel disease.* Human Brain Mapping, 2021. **42**(4): p. 993-1002.
245. Grimmer, T., et al., *White matter hyperintensities predict amyloid increase in Alzheimer's disease.* Neurobiology of aging, 2012. **33**(12): p. 2766-2773.
246. Vipin, A., et al., *Cerebrovascular disease influences functional and structural network connectivity in patients with amnestic mild cognitive impairment and Alzheimer's disease.* Alzheimer's research & therapy, 2018. **10**(1): p. 1-15.
247. Chong, J.S.X., et al., *Influence of cerebrovascular disease on brain networks in prodromal and clinical Alzheimer's disease.* Brain, 2017. **140**(11): p. 3012-3022.
248. Kandel, B.M., et al., *White matter hyperintensities are more highly associated with preclinical Alzheimer's disease than imaging and cognitive markers of neurodegeneration.* Alzheimer's & Dementia: Diagnosis, Assessment & Disease Monitoring, 2016. **4**: p. 18-27.

CURRICULUM VITAE

Doaa Ali, M.D., MSc

Education and Post-graduate Training

INSTITUTION AND LOCATION	DEGREE	Starting Date	Completion Date	FIELD OF STUDY
Faculty of Medicine, Tanta University Tanta, Egypt	MD	09/2004	02/2011	Medicine
Department of Internal Medicine and Department of Surgery Tanta University Hospitals, Tanta, Egypt	Internship	03/2011	02/2012	Medicine – Surgery
Faculty of Medicine, Tanta University, Egypt	MSc	10/2012	04/2015	Master's Degree in Neurology and Psychiatry
Department of Behavioral Science, College of Medicine, University of Kentucky	PhD student	01/2020	present	Clinical and Translational science

Professional Position

2012 – 2014: Resident, Neurology and Psychiatry department, Faculty of Medicine, Tanta University.

2014 – 2015: Chief Resident of Neurology and Psychiatry, Department of Neurology and Psychiatry, Tanta University Hospitals, Tanta, Egypt

2015 – 2019: Assistant Lecturer of Neurology and Psychiatry, Tanta University, Egypt

2019 – 2020: Research Assistant, Sanders Brown Center on Aging, University of Kentucky

2020 – 2023: Graduate Research Assistant, Sanders Brown Center on Aging, University of Kentucky

2023 – present: Imaging Research Scientist, Sanders Brown Center on Aging, University of Kentucky

<div align="center">

Professional Membership

</div>

08/2018 - ongoing American Academy of Neurology

06/2012 – ongoing Egyptian Society of Neurology

08/2010 – 12/2015 Member Egyptian White Coat Association (Medical Charity)

<div align="center">

Awards & Recognitions

</div>

06/2015 – Honors Degree Award – For MSc thesis entitled "Study of the psychiatric impact of political unrest on a sample of students at Tanta university"

03/2012 – Graduated Medical School with Honors Degree

<div align="center">

Scientific Publications:

</div>

a. **Ali DG**, Abner EL, Bahrani AA, El Khouli R, Gold BT, Jiang Y, Wilcock DM, Jicha GA. Amyloid-PET and White Matter Hyperintensities Have Independent Effects on

Baseline Cognitive Function and Synergistic Effects on Longitudinal Executive Function. Brain Sciences. 2023;13(2):218.

b. **Ali DG**, Bahrani AA, Barber JM, El Khouli RH, Gold BT, Harp JP, Jiang Y, Wilcock DM, Jicha GA. Amyloid-PET levels in the precuneus and posterior cingulate cortices are associated with executive function scores in preclinical Alzheimer's disease prior to overt global amyloid positivity. Journal of Alzheimer's Disease. 2022(Preprint):1-9.

c. Moga DC, Abner E, Schmitt F, Eckmann L, Huffmyer M, Martinez A, Beech B, George R, El Khouli R, **Ali D**. Intervention for Cognitive Reserve Enhancement in Delaying the Onset of Alzheimer's Symptomatic Expression (INCREASE) Study: Results from a Randomized Controlled Study of Medication Therapy Management Targeting a Delay in Prodromal Dementia Symptom Progression. The Journal of Prevention of Alzheimer's Disease. 2022;9(4):646-54.

Conference Abstracts and Presentations:

International Conferences:

1. "Cognitive reserve for memory performance is mediated by preclinical frontotemporal and limbic amyloid deposition in subjects with normal cognition in early MCI"

   Doaa Ali, Daniela Moga, Riham El-Khouli, Ashely Martinez, Erin Abner, and Gregory Jicha Alzheimer's Association International Conference 2020 (AAIC 2020)

2. "Preclinical amyloid-PET SUVr in the precuneus and posterior cingulate associations with MoCA scores are driven by language domain subscores"

   Doaa Ali, Justin M Barber, Riham H El Khouli, Brian T. Gold, Jordan Harp, Linda J Van Eldik, Donna M Wilcock, Gregory A Jicha. Alzheimer's Association International Conference 2021 (AAIC 2021)

3. "Executive dysfunction is the earliest sign of preclinical Alzheimer's disease detected by regional Ab-PET SUVr in the precuneus and posterior cingulate cortex"

   Doaa Ali, Justin M. Barber, Riham H. El Khouli, Brian T. Gold, Jordan Harp, Linda J. Van Eldik, Donna M. Wilcock, Gregory A. Jicha. Alzheimer's Association International Conference 2021 (AAIC 2021)

4. "Does targeted medication therapy management increase cognitive reserve? Results from the INtervention for Cognitive Reserve Enhancement in delaying the onset of Alzheimer's Symptomatic Expression (INCREASE) study"

Daniela C Moga, Erin L Abner, Frederick A Schmitt, Lynne Eckmann, Mark Huffmyer, Ashley I Martinez, Brooke F Beech, Rosmy George, Riham H El Khouli, **Doaa Ali**, Gregory A Jicha . Alzheimer's Association International Conference 2021 (AAIC 2021)

5. "Longitudinal plasma Alzheimer's disease biomarkers in an Alzheimer's disease research center cohort suggest pTau181 as the most reliable plasma biomarker for brain Alzheimer's pathology"

Tiffany L. Sudduth, Zachary Winder, Frederick A. Schmitt, Jordan Harp, Peter T. Nelson, **Doaa Ali**, Gregory A. Jicha, Donna M. Wilcock. Alzheimer's Association International Conference 2021 (AAIC 2021)

6. "The Combined Effect of β-Amyloid and White Matter Hyperintensities on Present and Future Executive Function Performance in Cognitively Normal Older Adults"

Doaa Ali, Riham H El Khouli, Erin L Abner, Ahmed Bahrani, Brian T. Gold, Yang Jiang, Donna M Wilcock, and Gregory A Jicha. Alzheimer's Association International Conference 2022 (AAIC 2022)

7. "Discrete white matter hyperintensity (WMH) growth quantification is superior to measurements of total longitudinal WMH volume change: implications for clinical trials in VCID"

Ahmed Ali Bahrani, Justin M Barber, Brian T. Gold, **Doaa Ali**, David K Powell, Linda J Van Eldik, Larry B Goldstein, Donna M Wilcock, Gregory A Jicha. Alzheimer's Association International Conference 2022 (AAIC 2022)

National Conferences:

"F-18 Amyvid PET CT In Asymptomatic Patients: Manual Versus Automated Analysis And Association With Patients' Global Cognitive Function."

Doaa G Ali, Daniela C Moga, Riham H. El Khouli, Gregory A. Jicha. Radiology society of North America 2021 (RSNA 2021) Chicago, IL